Transcriptomics reveals the putative mycoparasitic strategy of the mushroom *Entoloma abortivum* on species of the mushroom *Armillaria*

Running title: Mycoparasitism of *Armillaria* species by *Entoloma abortivum*

Rachel A. Koch[1] and Joshua R. Herr[1,2,#]

[1]Department of Plant Pathology, University of Nebraska, Lincoln, NE 68503, USA;

[2]Center for Plant Science Innovation, University of Nebraska, Lincoln, NE 68588, USA;

[#]Correspondence: Joshua R. Herr (jherr@unl.edu)

Abstract word count (including abstract and importance): 363

Text word count: 4938

ABSTRACT

During mycoparasitism, a fungus—the host—is parasitized by another fungus—the mycoparasite. The genetic underpinnings of these relationships have been best characterized in ascomycete fungi. However, within basidiomycete fungi, there are rare instances of mushroom-forming species parasitizing the reproductive structures, or sporocarps, of other mushroom-forming species, which have been rarely investigated on a genetic level. One of the most enigmatic of these occurs between *Entoloma abortivum* and species of *Armillaria*, where hyphae of *E. abortivum* are hypothesized to disrupt the development of *Armillaria* sporocarps, resulting in the formation of carpophoroids. However, it remains unknown whether carpophoroids are the direct result of a mycoparasitic relationship. To address the nature of this unique interaction, we analyzed gene expression of field-collected *Armillaria* and *E. abortivum* sporocarps and carpophoroids. Transcripts in the carpophoroids are primarily from *E. abortivum*, supporting the hypothesis that this species is parasitizing *Armillaria*. Most notably, we identified differentially upregulated *E. abortivum* β-trefoil-type lectins in the carpophoroid, which we hypothesize bind to *Armillaria* cell wall galactomannoproteins, thereby mediating recognition between the mycoparasite and the host. The most differentially upregulated *E. abortivum* transcripts in the carpophoroid code for oxalate decarboxylases—enzymes that degrade oxalic acid. Oxalic acid is a virulence factor in many plant pathogens, including *Armillaria* species, however, *E. abortivum* has evolved a sophisticated strategy to overcome this defense mechanism. The number of gene models and genes that code for carbohydrate-active enzymes in the *E. abortivum*

transcriptome were reduced compared to other closely related species, perhaps as a result of the specialized nature of this interaction.

IMPORTANCE

By studying fungi that parasitize other fungi, we can understand the basic biology of these unique interactions. Studies focused on the genetic mechanisms regulating mycoparasitism between host and parasite have thus far concentrated on a single fungal lineage within the Ascomycota. The work presented here expands our understanding of mycoparasitic relationships to the Basidiomycota and represents the first transcriptomic study to our knowledge that examines fungal-fungal relationships in their natural setting. The results presented here suggest that even distantly related mycoparasites utilize similar mechanisms to parasitize their host. Given that species of the mushroom-forming pathogen *Armillaria* cause plant root-rot diseases in many agroecosystems, an enhanced understanding of this interaction may contribute to better control of these diseases through biocontrol applications.

INTRODUCTION

Fungal mycoparasitism is a nutritional strategy where a living fungus – the host – is parasitized by and acts as a nutrient source for another fungus – the mycoparasite. Certain species of fungi in the Hypocreales (Ascomycota) are among the best-studied mycoparasites. Perhaps the most well-known of these are species of *Trichoderma* and *Clonostachys rosea*, which have biocontrol activity against plant pathogenic species of *Botrytis*, *Fusarium*, *Pythium*, and *Rhizoctonia* (1, 2). Other fungal mycoparasites in the Hypocreales include *Tolypocladium* species, many of which are parasites on the reproductive structures, or sporocarps, of species in the genus *Elaphomyces* (Eurotiales, Ascomycota) (3), *Escovopsis weberi*, which is a specialized necrotrophic parasite of fungal gardens of attine ants (4, 5) and *Hypomyces lactiflurum*, which parasitizes the mushrooms of *Russula* species and transforms them into the iconic "lobster mushroom" (6). Within the Basidiomycota, a well-studied genus of mycoparasites include *Tremella* species, which are parasites of corticiaceous basidiomycetes (7) and lichen-forming fungi (8).

Less studied examples of mycoparasitism involve mushroom-forming fungi that parasitize other mushroom-forming fungi. Fewer than 20 reported mushroom species may engage in this type of interaction, making it an incredibly rare phenomenon given the total number of mushroom-forming fungi (9, 10). Examples of this interaction whereby the parasite does not appear to impact the fitness of the host include *Volvariella surrecta*, which fruits from the pileus of its host, *Clitocybe nebularis* (11), and *Asterophora* species, which colonize their *Russula* or *Lactarius* host after it dies (10). More commonly, though, mushroom mycoparasites deform host sporocarps and likely

93 prevent the dispersal of their spores. *Pseudoboletus parasiticus* fruits from the
94 sporocarps of *Scleroderma* species, which, after infection, are no longer able to mature
95 and disperse their spores (12). *Psathyrella epimyces* causes the deformation of
96 sporocarp tissue of its host, *Coprinus comatus* (13). Additionally, of the ten mushroom
97 species in the genus *Squamanita*, all are known to be parasites of sporocarps of
98 species in the genera *Cystoderma*, *Galerina*, *Hebeloma*, and *Inocybe* (10).

99 One of the most frequently encountered putative mycoparasitic interactions
100 between two mushrooms involves species of *Armillaria* and *Entoloma abortivum* (Fig.
101 1). *Entoloma abortivum* is often encountered fruiting in soil, humus, or decaying logs in
102 deciduous woods (14), while *Armillaria* species are facultative necrotrophs that can
103 cause root rot in forest and agronomic systems worldwide (15, 16). *Entoloma abortivum*
104 was originally described to occur as two morphologies: the mushroom form, which has a
105 pinkish-gray stipe and pileus, and pink gills, and then the carpophoroid form, which is
106 generally white and subglobose, and does not develop well-formed gills (Fig. 1). Initially,
107 the carpophoroid form was assumed to be *E. abortivum* sporocarps that were
108 malformed due to parasitism by *Armillaria* species (14). However, macro- and
109 microscopic studies of carpophoroid collections determined that they are actually
110 *Armillaria* sporocarps permeated with *E. abortivum* hyphae (17). Laboratory inoculation
111 experiments showed that *E. abortivum* interacts with *Armillaria* sporocarps to disrupt
112 their morphological development (17).

113 Whether carpophoroids are the result of a mycoparasitic relationship, where *E.*
114 *abortivum* serves as the mycoparasite and *Armillaria* species serve as the host, remains
115 unknown. To address this, we initiated a transcriptome study after we encountered all

116 three components of this system fruiting in close proximity—carpophoroids and
117 individual sporocarps of *E. abortivum* and *Armillaria*. For a mycoparasite to be
118 successful, there are several crucial steps to the utilization of a fungal host for nutrition.
119 These steps include: 1) sensing the host; 2) recognition and attachment to host hypha;
120 3) initiating defense responses; and 4) the eventual demise of the host (18). Previous
121 genomic and transcriptomic studies elucidated the genetic machinery that model
122 mycoparasites utilize during each of these steps (18–20). In this work, we used
123 transcriptomic and meta-transcriptomic techniques to analyze the genomic toolbox of *E.*
124 *abortivum* and *Armillaria* during the carpophoroid stage. We show that the gene
125 expression profiles of *E. abortivum* resemble those of known mycoparasitic species, as
126 well as predict certain genes in both species that facilitate this interaction. Additionally,
127 we used transcriptomic information to determine the species of *Armillaria* involved in
128 this association.
129

130 **RESULTS**

131 ***Transcriptome assemblies of* Entoloma abortivum *and* Armillaria*.*** To benchmark
132 gene diversity and baseline expression levels of the field-collected mushroom species in
133 our study, we sequenced the sporocarp transcriptomes of *E. abortivum* and the
134 *Armillaria* species found in close proximity to the carpophoroids. To date, there are
135 several transcriptomic studies of *Armillaria* species (21, 22), but none for any *Entoloma*
136 species. The assembled transcriptome of *E. abortivum* was just under 120 million base
137 pairs. There were a total of 43,599 contigs and an N50 value of 3,527; 94.5% of
138 benchmark universal single-copy orthologs (BUSCOs) from the Agaricales were present

139 in the *E. abortivum* transcriptome. Nine internal transcribed spacer (ITS) sequences
140 were extracted from the transcriptome, accounting for 5.96×10^{-4} % to 1.82×10^{-3} % of the
141 mapped reads; all ITS sequences were from *E. abortivum*. Within the contigs, a total of
142 9,728 unique gene models were recovered in the transcriptome assembly (Fig. 2) with
143 603 transcripts differentially upregulated in the carpophoroid tissue when compared to
144 the sporocarp tissue and 403 transcripts differentially upregulated in the sporocarp
145 tissue when compared to carpophoroid tissue (Fig. 3). The transcriptome contained 195
146 genes that code for carbohydrate-active enzymes (CAZymes). The transcriptome lacks
147 any genes that code for cellobiohydrolases (glycoside hydrolase (GH) 6 and GH7),
148 xylanases (GH10, GH11, GH30) and auxiliary proteins like polysaccharide
149 monooxygenases (GH61) but does contain nine chitinases (GH18) (Fig. 2). Transcripts
150 detected in the *E. abortivum* transcriptome that were previously determined to play
151 important roles in mycoparasitic interactions (18–20) include: ten putative secondary
152 metabolite gene clusters, one G-coupled protein receptor (GCPR), 38 ATP-binding
153 cassette (ABC) transporters and 113 genes from the major facilitator superfamily (MFS)
154 (Fig. 3). The average gene expression (in normalized units of trimmed mean of m-
155 values (TMM)) of the ten most abundant *E. abortivum* transcripts in the sporocarp
156 ranged from 4,333 to 17,890. Information about the ten most abundant transcripts in the
157 sporocarps is available in Table 1.

158 The assembled transcriptome of *Armillaria* was just over 138 million base pairs.
159 A total of 63,905 contigs, an N50 value of 2,845, and 97.8% of the BUSCOs
160 representative of the Agaricales were present in the transcriptome. Eleven ITS
161 sequences were extracted from the transcriptome, accounting for 2.77×10^{-5} % to

162 6.26×10^{-4} % of the mapped reads; six ITS sequences were from *Armillaria*, while five
163 were from an uncharacterized species of the yeast *Kodamaea*. A total of 38,215 unique
164 gene models were recovered, and, after bioinformatic filtering against public Armillaria
165 genomes, 29,936 of these representing orthologs of *Armillaria* species (Fig. 2). In total,
166 2,619 transcripts were differentially upregulated in the carpophoroid tissue when
167 compared to the sporocarp tissue, whereas 9,820 transcripts were differentially
168 upregulated in the sporocarp tissue when compared to the carpophoroid tissue (Fig. 3).
169 The transcriptome contained 580 genes that code for CAZymes, with 34 of those coding
170 for chitinases (Fig. 2). Genes detected in the *Armillaria* transcriptome that might be
171 important in mycoparasitic interactions include: 12 putative secondary metabolite gene
172 clusters, five GCPRs, 59 ABC transporters and 144 MFS transcripts (Fig. 3). The
173 average TMM of the ten most highly upregulated *Armillaria* transcripts in the sporocarp
174 ranged from 8,438 to 36,477. The most differentially upregulated transcript was
175 annotated as a cell wall galactomannoprotein (Fig. 4 and 5) (Table 2), while, notably,
176 the fourteenth most differentially upregulated transcript in the sporocarp coded for
177 isocitrate lyase (Table 2, Fig. 5).
178
179 **Metatranscriptomic analysis of combined fungal hyphae in carpophoroid tissue.**
180 We sequenced the metatranscriptome of the mixed tissue in the carpophoroids that are
181 typically found when *E. abortivum* and species of *Armillaria* are found in proximity. In the
182 carpophoroid tissue, significantly more transcriptomic reads from *E. abortivum* were
183 identified than from *Armillaria* sp. ($t_{(8)} = 16.6$, $p = 1.77\times10^{-7}$, $n = 9$ replicates per species)
184 (Fig. 6). The average number of *E. abortivum* mapped reads in the carpophoroid tissue

185 was 2,613,988, while the average number of *Armillaria* mapped reads was 74,880 (Fig.
186 6).

187 The average TMM of the top ten most abundant *E. abortivum* transcripts in the
188 carpophoroid ranged from 9,075 to 68,720 (Table 1), while the average TMM of the top
189 ten most differentially upregulated *Armillaria* transcripts in the carpophoroid ranged from
190 300 to 9,049 (Table 2). The first and third most highly upregulated *E. abortivum*
191 transcripts in the carpophoroid tissue code for two oxalate decarboxylases, both of
192 which were differentially upregulated in the carpophoroid tissue compared to the
193 sporocarp (Figs. 3, 4, 5 and Table 1). There were other differentially upregulated *E.*
194 *abortivum* transcripts in the carpophoroid that were not as highly upregulated that may
195 also play a role in mycoparasitism. These include three β-trefoil-type lectins, three ABC
196 transporters, two chitinases, and 14 MFS transcripts (Fig. 3, Table 1). We were unable
197 to detect any transcripts involved in secondary metabolite gene clusters that were
198 differentially upregulated in the carpophoroids (Fig. 3). Two *Armillaria* transcripts coding
199 for putative senescence-associated proteins, as well as a heat shock protein associated
200 with cell death, were differentially upregulated in the carpophoroid compared to the
201 sporocarp (Table 2).

202

203 ***Phylogenetic placement of* Armillaria *reads.*** Phylogenomic analysis of 100 *Armillaria*
204 BUSCOs generated in this study, in conjunction with previously published *Armillaria*
205 genomes, shows a strongly supported sister relationship with an *A. mellea* specimen
206 from France (100% BS) (Fig. 7A). Phylogenetic analysis of all ITS sequences

207 characterized as *A. mellea* from GenBank shows that this specimen is conspecific with
208 specimens from eastern North America (Fig. 7B).
209
210 **DISCUSSION**
211 The formation of carpophoroids associated with species of *E. abortivum* have
212 traditionally been thought to be the result of an *Armillaria* species attacking and
213 parasitizing *Entoloma* sporocarps (14), hypothesized on the basis that *Armillaria* are
214 wide-spread generalist forest pathogens that exhibit a broad range of host plants (15).
215 However, subsequent studies suggested the opposite: the production of carpophoroids
216 are the result of *E. abortivum* disrupting the development of *Armillaria* sporocarps (17).
217 Here, we employed RNA sequencing and differential gene expression analysis on field-
218 collected fungal tissue of each of the three components of this association to better
219 understand the mechanistic basis of this interaction. We determined that *E. abortivum*
220 reads in the metatranscriptome of the carpophoroid tissue—which can be interpreted as
221 a measure of living tissue—are almost 35 times more abundant than *A. mellea* reads
222 (Fig. 6). This finding suggests that carpophoroids are structures that result from *E.*
223 *abortivum* parasitizing, and eventually killing, its *Armillaria* host under natural conditions.
224 Fungal-fungal necrotrophic mycoparasitic interactions are multistage processes
225 that are best studied in model species, such as those in the genera *Trichoderma*,
226 *Coniothyrium, Clonostachys* and *Tolypocladium* (20). Genomic and transcriptomic
227 studies of necrotrophic mycoparasites show a convergence of significant genetic
228 mechanisms at each stage (20). The *E. abortivum* genes that are differentially
229 upregulated in the carpophoroid tissue are largely consistent with other examples of

230 necrotrophic mycoparasites in the Ascomycota. In the carpophoroid tissues we
231 analyzed, *E. abortivum* appears to employ much of its energy on recognition and
232 defense responses (Fig. 5). Inversely, the *Armillaria* sporocarps we analyzed illuminate
233 possible mechanisms by which these two species recognize one another and how
234 *Armillaria* responds to parasitism (Fig. 5).
235
236 ***The genetics of the* Entoloma-Armillaria *mycoparasitic interaction.*** A crucial step in
237 a successful mycoparasite's life history is the ability to sense its host. Genes involved in
238 the recognition of the fungal prey include those that code for GPCRs (18, 20). However,
239 we did not find any of these genes that were differentially upregulated by *E. abortivum*
240 in the carpophoroid tissue (Fig. 3). Given the significantly fewer number of *Armillaria*
241 reads in the carpophoroid tissue compared to *E. abortivum*, we presume that these
242 carpophoroids are relatively advanced in age, and expression of the genes used for
243 sensing the presence of the host are no longer necessary.
244 We also identified three *E. abortivum* transcripts that code for β-trefoil-type
245 lectins—proteins that bind to galactose units of sugar chains (23)—that were
246 differentially upregulated in the carpophoroid tissue (Figs. 3 and 5). In well-studied
247 mycoparasitic interactions, the recognition, attachment, and coiling around a fungal
248 substrate is mediated by lectins expressed by at least one of the fungal partners (24–
249 26). More specifically, basidiomycete β-trefoil-type lectins have previously been shown
250 to play a role in the recognition of non-self glycans (27). Interestingly, the most
251 abundant and differentially upregulated transcript produced in the *Armillaria* sporocarps,
252 the substrate to which *E. abortivum* hyphae attach, codes for a cell wall

253 galactomannoprotein (Figs. 4 and 5). These proteins belong to a group of glycans which
254 consist of a mannose backbone with galactose side chains and are known to make up a
255 major part of the cell wall of some fungal species (28). This particular
256 galactomannoprotein appears to be specific to *Armillaria* species. Watling (14)
257 commented on the highly specific nature of this interaction and that it has only been
258 documented occurring between *E. abortivum* and *Armillaria* species. One possible
259 mediator of the specificity of this interaction could be the galactose sugars on the
260 mannose protein (only known thus far from *Armillaria* species) that are the means by
261 which *E. abortivum* β-trefoil-type lectins recognize and attach to its *Armillaria* host.
262 However, more genome sequencing of other Agaricales species is needed to determine
263 whether this protein is truly specific to species in the genus *Armillaria*.
264 During mycoparasitic interactions, the fungal host responds by mounting its own
265 defense, and a successful mycoparasite must be able to cope with this counterattack
266 (18, 20). Oxalic acid is a virulence factor employed by some plant pathogens, including
267 species of *Armillaria*, to compromise the defense responses of the host plant by
268 creating an acidic environment (29, 30). One differentially upregulated *Armillaria*
269 transcript in the sporocarps codes for isocitrate lyase (Fig. 5), which is involved in OA
270 biosynthesis in other fungal pathogens (31, 32), and we suspect that *Armillaria*
271 sporocarps may utilize OA to defend against the initial infection by *E. abortivum*.
272 However, two of the most abundant and differentially upregulated *E. abortivum*
273 transcripts in the carpophoroid tissue code for oxalate decarboxylases—enzymes
274 responsible for the degradation of OA (Figs. 3, 4, 5D, Table 1). In at least one known
275 well-studied mycoparasitic interaction, OA is secreted by the fungal host, *Sclerotinia*

276 *sclerotiorum*, in reaction to penetration by its mycoparasite, *Coniothyrium minitans*. The
277 acidic environment created by the secreted OA inhibits conidial germination and
278 suppresses mycelial growth of *C. minitans* (33). However, *C. minitans* nullifies the
279 growth-suppressing effects of OA or OA-mediated low pH by degrading the OA (34, 35),
280 an enzymatic process largely mediated by oxalate decarboxylase. Because of this,
281 oxalate decarboxylase plays an imperative role in mycoparasitism as OA degradation is
282 vital for infection of the fungal host (36). Given the abundance of these genes produced
283 by *E. abortivum* in the carpophoroid, we suspect a similar scenario in this mycoparasitic
284 interaction. Subsequent downregulation of isocitrate lyase by *Armillaria* in the
285 carpophoroids suggests that its genetic defense responses to infection were likely over
286 at the time of our sampling.

287 Other ways that mycoparasites cope with the counterattack launched by their
288 host include actively excreting host-secreted toxins. Here, we hypothesize that active
289 extrusion of toxins secreted by the host occurs in the *E. abortivum* carpophoroid tissue
290 via membrane transporters in the ABC superfamily (37–39). Three ABC transporters
291 were differentially upregulated in the carpophoroid tissue (Fig. 3). Another group of
292 genes that were differentially upregulated by *E. abortivum* in the carpophoroid belong to
293 the major facilitator superfamily (MFS) transporters (Fig. 3). In *C. rosea*, there was
294 selection for genes in this family that were related to drug resistance, and the transport
295 of secondary metabolites, small organic compounds and carbohydrates (40). Their
296 importance to mycoparasitism in *C. rosea* is predicted to invoke efflux-mediated
297 protection against exogenous or endogenous secondary metabolites and nutrient
298 uptake (40). MFS transporters have also been shown to be induced in other

299 mycoparasitic species (19, 41), but their exact biological roles have not been
300 investigated.

301 In mycoparasitism, the final death of the host often results from the synergistic
302 actions of cell wall-hydrolytic enzymes and antifungal secondary metabolites (18, 20).
303 No secondary metabolite gene clusters identified in the *E. abortivum* transcriptome were
304 differentially upregulated in the carpophoroid tissue (Fig. 3). In some mycoparasitic
305 relationships, the secretion of secondary metabolites occurs early in the interaction,
306 including in *Escovopsis weberi*, which secretes toxic compounds that kill the leafcutter
307 ant garden before contact (5). In culture experiments between *Armillaria* isolates and *E.*
308 *abortivum*, the growth of *Armillaria* was severely inhibited by the presence of *E.*
309 *abortivum* (42). This suggests that *E. abortivum* may potentially secrete a toxic
310 compound early in the interaction that inhibits the growth of *Armillaria*. Given that
311 significantly more of the living tissue in the carpophoroids belonged to *E. abortivum* (Fig.
312 6), it is possible that much of the *Armillaria* tissue was killed preceding the full
313 development of the carpophoroid.

314 Additionally, we hypothesize that the upregulated β-trefoil-type lectin in *E.*
315 *abortivum* that may be important in hyphal recognition may also be cytotoxic towards
316 *Armillaria*. This type of lectin has sequence homology, as well as putative structural
317 similarity, to the B-subunit of ricin, a toxic protein from the castor bean *Ricinus*
318 *communis* (43). An array of β-trefoil-type lectins have been characterized from the
319 sporocarps of the mushroom-forming species *Clitocybe nebularis* (44), *Coprinus cinerea*
320 (27), *Macrolepiota procera* (45) and *Boletus edulis* (46). Besides being important for
321 non-self recognition, these same mushroom lectins also exhibit entomotoxic activity (47)

322 as well as nematoxic activity (27, 45, 48). Taken together, it is possible that the *E.*
323 *abortivum* β-trefoil-type lectins may also function as toxins towards *Armillaria*. While the
324 *E. abortivum* transcripts coding for these lectins are not in the highest abundance in the
325 carpophoroid tissue (Fig. 5), this could be because most of the *Armillaria* sporocarp
326 tissue is already dead and the potential lethal effects produced by them are no longer
327 necessary.

328 Chitin is an essential polymer in fungal cell walls (49) and is an important target
329 during mycoparasitic attack (20). Indicative of the importance of chitinases in
330 mycoparasitic interactions, members of the genus *Trichoderma*, as well as
331 *Tolypocladium ophioglossoides* and *Escovopsis weberi,* have an increased number of
332 genes coding for them (19, 50–53). Nine fungal chitinases were detected in the
333 transcriptome of *E. abortivum*, which is fewer than the 13, 19, 20 and 29 detected in the
334 closely related species, *Tricholoma matsutake* (54)*, Clitocybe gibba* (55)*, Lyophyllum*
335 *atratum* (56) and *Lepista nuda* (55), respectively (Fig. 2). Only two of those *E. abortivum*
336 chitinases were differentially upregulated in the carpophoroid tissue (Fig. 3) and were
337 not abundant in comparison to other genes, suggesting minimal significance at this
338 stage in carpophoroid development. One possibility for this difference in abundance
339 could be the result of the putatively acidic pH in the carpophoroid that we infer based on
340 the high gene expression of oxalate decarboxylases. In *C. minitans*, chitinase activity is
341 positively correlated with ambient pH ranging from three to eight (57), so it is possible
342 that chitinase activity in *E. abortivum* will increase after a neutral pH is restored. Another
343 possibility for the low abundance is that most of the *Armillaria* host tissue was already
344 broken down, reducing the need for chitinase activity.

345 Some of the putatively mycoparasitism-related genes outlined above were also
346 differentially upregulated by *Armillaria* in the carpophoroid tissue. These include genes
347 that code for MFS, ABC transporters, chitinases, and secondary metabolite gene
348 clusters (Fig. 3). This suggests that *Armillaria* may be using many of the same genetic
349 mechanisms to defend itself against parasitism by *E. abortivum*. Additionally, the degree
350 of expression changes—both in the number of differentially upregulated transcripts and
351 the log-fold change (logFC)—between the sporocarp and carpophoroid is much greater
352 in *Armillaria* compared to *E. abortivum* (Fig. 3, 4), which could reflect an increase in the
353 level of defense from *Armillaria*. However, this defense is apparently not enough to
354 overcome the parasitic adaptations of *E. abortivum*.
355
356 ***Gene and CAZyme content of* E. abortivum*.*** The number of predicted gene models in
357 the transcriptome of *E. abortivum* was 9,728, which is markedly fewer than the number
358 of gene models in the genomes of its closest sequenced relatives (Fig. 2B). Additionally,
359 relative to other closely related mushroom species, *E. abortivum* also exhibits a strong
360 reduction in several gene families encoding CAZymes (Fig. 2C), and contains no
361 cellobiohydrolases, xylanases, or polysaccharide monooxygenases. This finding is
362 consistent with what has been observed in obligate mycoparasites and animal
363 pathogens, which also have reduced CAZyme repertoires compared to fungi that utilize
364 other nutritional strategies, hypothesized to be the result of their highly specialized
365 interactions with their hosts (50, 58, 59). Therefore, it is possible that *E. abortivum* only
366 retained the CAZymes and accessory genes necessary to interact with *Armillaria*
367 species. While a genome sequence of *E. abortivum* will be necessary to confirm this

368 reduction, the BUSCO analysis verified that the *E. abortivum* transcriptome contains
369 nearly 95% of the core set of eukaryotic genes, which suggests that our transcriptome is
370 relatively complete, and it is unlikely that entire gene families are underrepresented.
371 Another possibility for the reduction in CAZymes could be explained by a broader
372 nutritional strategy employed by *Entoloma* species, some of which form ectomycorrhiza-
373 like structures on host plant species (60–62). Ectomycorrhizal species have a marked
374 reduction in CAZymes in comparison to their saprotrophic ancestors (63), which we also
375 observe with *Tricholoma matsutake* (Fig. 2C). However, microscopic analyses of
376 *Entoloma* ectomycorrhizae-like structures suggest that some species destroy root
377 meristems and young root cells, suggestive of a more parasitic relationship (60, 61).
378 One explanation is that *Entoloma* species, in general, are parasites of true
379 ectomycorrhizae. More broadly, other species within the Entolomataceae are suspected
380 mycoparasites, as they have been reported growing in close association with the
381 sporocarps of other species (reviewed in (17)), including *Entoloma parasiticum*
382 (=*Claudopus parasiticus*) and *Clitopilus fasciculatus* (64, 65). This explanation would
383 also add credence to the evidence that Entolomataceae species are difficult to culture
384 and are slow growing (62). Additional research utilizing genomes and laboratory studies
385 to understand the nutritional strategy employed by this lineage will inform us as to
386 whether fungal parasitism in this group is more common than it is currently understood
387 to be. Lastly, it should be noted that *Entoloma* species, and *E. abortivum* in particular,
388 form sclerotia in culture and presumably in soil (14, 17). These resting structures are
389 perhaps a dormancy mechanism in the soil to survive seasonality when host tissue is
390 unavailable. Because the timing and presence of *E. abortivum* fruitings have been hard

391 to predict, we were not able to observe or acquire a transcriptome for the sclerotia in the
392 field.
393
394 ***Gene content and identity of* Armillaria *species in this interaction.*** The number of
395 predicted gene models in the transcriptome of this *Armillaria* species was 38,215 (Fig.
396 2B). This is substantially greater than all other sequenced *Armillaria* species, which
397 range from 14,473 to 25,704 gene models (22, 66). However, when we looked for gene
398 models in our transcriptome that belong to known *Armillaria* species, this reduced the
399 total number of gene models to 29,936 (Fig. 2B). The excess gene models in the
400 *Armillaria* transcriptome, when compared to reference genomes, likely represent
401 duplicated gene models with splice variants, a common artifact of transcriptome
402 sequencing (67). Additionally, nearly one quarter of the gene models in the *Armillaria*
403 sporocarps were from organisms other than *Armillaria*, including the yeast *Kodamaea*,
404 highlighting the fact that field-collected sporocarps are not composed of tissue from a
405 single organism. However, none of these contaminating organisms had genes that were
406 both abundant and differentially upregulated that we predicted to play a role in this
407 interaction.
408 Phylogenomic analysis of the *Armillaria* transcripts generated in this study
409 suggest that the specific *Armillaria* species parasitized in this relationship is sister to an
410 *A. mellea* specimen collected from western Europe (Fig. 7A). An ITS-based
411 phylogenetic analysis shows the *Armillaria* specimen collected in this study is
412 conspecific with other *A. mellea* collections from eastern North America (Fig. 7B).
413 Before now, observations of *A. mellea sensu stricto.* fruiting in proximity to

414 carpophoroids (17) hinted it may be a host to *E. abortivum*. Herein, though, we show for
415 the first time using genomic data that *A. mellea s. s.* can definitively serve as a host for
416 *E. abortivum.* However, our hypothesis is that this interaction does not appear specific
417 to just *A. mellea s. s.*, as *A. gallica*, *A. ostoyae*, *A. jezoensis*, *A.* sp. Nag. E and
418 *Desarmillaria tabescens* have been previously confirmed as hosts in this interaction as
419 well (17, 42, 68). However, a broad geographic sampling of carpophoroids using
420 molecular markers or genomic information could address this question more thoroughly.
421 Interestingly, *Armillaria* species parasitized by *E. abortivum* appear to be only those
422 present in Eastern North America and Eastern Asia (17, 42, 68).
423
424 ***Conclusions.*** Data from this study support the hypothesis that *E. abortivum* is a
425 mycoparasite of *Armillaria* sporocarps. Three β-trefoil-type lectins are differentially
426 upregulated by *E. abortivum* in the carpophoroid tissue, and we propose that these
427 lectins mediate recognition with *Armillaria* sporocarps through binding to an *Armillaria*-
428 specific galactomannoprotein. We hypothesize that by using oxalate decarboxylase, *E.*
429 *abortivum* is likely defending against the secretion of OA by *Armillaria*. These strategies
430 employed by *E*. *abortivum* for recognition and defense are similar to mechanisms
431 utilized by other mycoparasites, suggesting that even distantly related mycoparasites
432 utilize similar genetic mechanisms to mediate mycoparasitic interactions. One
433 weakness of this study is that we were limited to the carpophoroid life stage that was
434 available at the point of collection, which led us to speculate about what is occurring
435 during other stages of mycoparasitism (i.e. sensing the host, initiating the interaction
436 and killing and consuming the host). Therefore, future studies using culture methods,

437 isotopic analysis and metatranscriptomics of naturally collected carpophoroids at
438 different life stages (i.e. younger and older carpophoroid specimens) will be necessary
439 to completely tease apart the putative mycoparasitic strategies employed by *E.*
440 *abortivum* and the defense responses by the *Armillaria* host. Finally, given that
441 *Armillaria* species are pathogens in both natural and agronomic systems, a better
442 understanding of this interaction may lead to the development of biocontrol methods for
443 the control of Armillaria root rot.
444

445 **MATERIALS AND METHODS**

446 **Sample collection, preparation, and sequencing.** Sporocarps of *Armillaria* sp., *E.*
447 *arbotivum*, and the mixed-tissue carpophoroids were observed fruiting in proximity to
448 one another on 18 September 2015 within the Baker Woodlot and Rajendra Neotropical
449 Migrant Bird Sanctuary, Michigan State University, East Lansing, MI 48823 (42°42'56.4"
450 N, 84°28'34.4" W) (collection accession: JRH 2446). Entire sporocarps were collected
451 and immediately flash frozen in liquid nitrogen and subsequently stored at -80°C. At the
452 time of processing, three biological replicates of each of the three tissue types
453 (*Armillaria sp*. sporocarp, *E. abortivum* sporocarp, and carpophoroid), were individually
454 ground in liquid N_2. Total RNA was then extracted from the ground tissue using the
455 Qiagen RNeasy kit (Qiagen Inc., Hilden, Germany) according to manufacturer's
456 protocol. RNA concentration and quality for each of the samples were assessed on a
457 DeNovix DS-11 FX Spectrophotometer (DeNovix Inc., Wilmington, DE 19810, USA) and
458 then shipped directly to the University of Minnesota's Genomics Center
459 (https://genomics.umn.edu). Three technical replicates were sequenced for each

460 biological replicate. Transcriptomic and metatranscriptomic libraries were constructed
461 with the TruSeq Standard Total RNA Library Preparation Kit with Ribo-Zero ribosomal
462 reduction following the protocol developed by Schuierer et al. (69). Nucleotide
463 sequencing was performed on the Illumina HiSeq 2500 System (Illumina Inc., San
464 Diego, USA) and paired-end RNA sequence reads of 51 bp were generated for further
465 analysis.
466
467 ***De novo transcriptome assembly, transcript abundance estimation and gene***
468 ***expression analysis.*** The quality of the raw reads was assessed using FastQC version
469 0.11.9 (https://www.bioinformatics.babraham.ac.uk/projects/fastqc). The range of the
470 number of reads for each condition are as follows: *E. abortivum* sporocarps ranged from
471 10,584,302 to 14,473,328; *Armillaria* sporocarps ranged from 11,712,320 to 12,431,979;
472 and the carpophoroids (containing reads from both organisms) ranged from 9,146,682
473 to 12,852,086. Sequencing adaptors were trimmed and PhiX contaminants were filtered
474 for each sample using bbduk (https://jgi.doe.gov/data-and-tools/bbtools/bb-tools-user-
475 guide/bbduk-guide/). Prior to transcriptome assembly, *k-mer* hash sizes were estimated
476 with *khmer* (70). De novo assemblies were constructed independently for both *Armillaria*
477 sp. and *E. arbotivum* with Trinity version 2.11.0 (71) using the trimmed reads generated
478 from the respective sporocarp reads. Assembly statistics for both transcriptomes were
479 generated with QUAST version 5 (72) and transcriptome completeness was assessed
480 by determining the percentage of sequenced BUSCOs in each (73).
481 The results of the *de novo* transcriptome assemblies were used as references to
482 perform sample-specific expression analysis. The trimmed sporocarp reads from each

483 of the nine replicates were mapped against their respective reference transcriptomes
484 using Bowtie 2 (74) followed by calculation of abundance estimates using RSEM (75).
485 The trimmed carpophoroid reads were also subsequently mapped, following the same
486 protocol as described above, to both the *Armillaria* sp. and *E. arbotivum* transcriptomes.
487 Because of the close phylogenetic relatedness between these two species, and to filter
488 out poorly aligned reads, we only retained mapped reads for all samples that had a
489 MAPQ value of 30 and above, which is equivalent to reads that have a 99.9% chance of
490 hitting the correct match. The R package edgeR (76) and "trimmed mean of M-value"
491 (TMM) normalization (77) were used to determine differentially upregulated transcripts
492 between: 1) *Armillaria* sporocarps and carpophoroids, and 2) *E. abortivum* sporocarps
493 and carpophoroids. Transcripts were considered differentially upregulated if they had a
494 logFC of two or greater and an FDR-adjusted *p*-value, or *q*-value, of < 0.05. All
495 statistical analyses for the packages listed above were conducted using R version 4.0.3
496 (http://www.r-project.org/).
497 We used SAMtools (78) to determine the number of reads from the
498 carpophoroids that mapped to our reference transcriptomes of *E. abortivum* and our
499 particular *Armillaria* species. To understand whether the number of reads that mapped
500 to the carpophoroids differed significantly between each fungal species, we performed
501 an *F*-test of equality of variances, and then a two-tailed *t*-test assuming unequal
502 variance with a *p*-value < 0.05 denoting significance.
503
504 ***Sporocarp Transcriptome and Carpophoroid Metatranscriptome Annotation.*** We
505 annotated the *Armillaria* sp. and *E. abortivum* transcriptomes using Trinotate version 3.2

506 (79). Briefly, the transcripts were translated to coding protein sequences using
507 TransDecoder version 5.5.0 (http://transdecoder.github.io) following identification of the
508 longest open reading frames. To identify the most likely homologous sequence data, we
509 used *blastx* on the transcripts and *blastp* on the predicted protein sequences (80). Using
510 the predicted protein sequences, we also ran a HMMER (81) search against the PFAM
511 database (82) to identify conserved domains that might be suggestive of function. We
512 also compared these results to currently curated annotation databases such as Gene
513 Ontology (GO) (83) and Kyoto Encyclopedia of Genes and Genomes (KEGG) (84–86).
514 We used dbCAN2 (87) to annotate the CAZymes present in both species and compared
515 their CAZy content to other closely related Agaricales species (22, 54–56), along with
516 antiSMASH version 5.0 (88) to identify transcripts that belong to secondary metabolite
517 gene clusters for both *Armillaria* and *E. abortivum*.
518 Finally, because this work was based off *de novo* transcriptome assemblies,
519 there was the possibility that transcripts from contaminating organisms, including
520 insects, yeasts, and other fungi, were also present and may be confounding the results.
521 We approached this issue multiple ways. First, we extracted all internal transcribed
522 spacer (ITS) regions from both transcriptomes, including the regions 18S, ITS1, 5.8S,
523 ITS2, and 28S, using ITSx (89), and identified the origin of those sequences. To verify
524 the number of mapped reads that represent rRNA, we also calculated the proportion of
525 reads that mapped to the transcripts that contained the ITS sequences to the total
526 number of mapped reads. Second, because high-quality genome assemblies of
527 *Armillaria* exist (22, 66), we used Exonerate (90) to determine how many of the gene
528 models in our *Armillaria* transcriptome are orthologs of *A. gallica*—the *Armillaria* species

529 with the largest number of known gene models. Finally, all genes that we report on as
530 important to this interaction were manually verified to be from the target organism—
531 *Armillaria* or *E. abortivum*—using the NCBI *blastx* tool (80) against the non-redundant
532 protein sequences database and confirming a hit from the Physalacriaceae or
533 Entolomataceae/Lyophyllaceae, respectively.
534
535 ***Phylogenetic analysis of* Armillaria *transcripts.*** In order to identify the specific
536 species of *Armillaria* associated in this relationship, we identified BUSCOs (73) from the
537 transcriptome of our *Armillaria* sporocarps along with other *Armillaria* and
538 Physalacriaceae species with previously sequenced genomes (22, 66, 91, 92). We
539 randomly selected 100 BUSCOs to reconstruct a phylogenomic tree from the six
540 *Armillaria* specimens (22, 66), *Guyanagaster necrorhizus* (92) and *Cylindrobasidium*
541 *torrendii* (91), which served as the outgroup. Protein-coding sequences were aligned
542 using MAFFT version 7 (93) and non-informative sites and non-aligning regions were
543 trimmed with Gblocks (94). The 100 BUSCOs were concatenated into a supermatrix
544 with 64,436 sites. This supermatrix was used to infer a species tree and branch support
545 using RAxML-NG (95), using a partitioned WAG+G model, where each data partition
546 represented an individual BUSCO.
547 To expand on the phylogenomic analysis above, we used the representative
548 *Armillaria* ITS sequence obtained from ITSx, and given the close relationship of our
549 *Armillaria* species to *A. mellea*, we pulled all *A. mellea* ITS sequences from GenBank
550 that included associated location metadata (96–110) (Table S1). These sequences
551 were aligned using MAFFT version 7 (93), with refinements to the alignment performed

552 manually. RAxML-NG (95) was used to reconstruct this phylogeny. Taxa used to root
553 this phylogeny included *A. gemina*, *A. sinapina*, *A. puiggarii* and *A. luteobubalina*—all
554 members of the sister lineage to *A. mellea fide* (16).
555
556 ***Data and code availability.*** The raw reads and assembled transcriptomes generated
557 during this study have been deposited in NCBI's Gene Expression Omnibus and are
558 accessible through GEO Series accession number GSE183699
559 (https://www.ncbi.nlm.nih.gov/geo/query/acc.cgi?acc=GSE183699) or under the NCBI
560 BioProject PRJNA761704. All other associated data, including analysis code and
561 information on voucher collections, are available at
562 https://github.com/HerrLab/Koch_Arma-Ento_2021.
563
564 **Acknowledgements**
565 We would like to give special thanks to Ben Lemmond and Eva Skific for providing
566 photos of this system and to Greg Bonito at Michigan State University for generously
567 storing sporocarp and carpophoroid tissue until we were able to transport the tissue to
568 our laboratory. We also want to thank three anonymous reviewers who provided
569 feedback and comments on the initial submission of this manuscript. This work was
570 completed using the Holland Computing Center of the University of Nebraska, which
571 receives support from the Nebraska Research Initiative. This research was directly
572 supported by start-up funding from the University of Nebraska Agricultural Research
573 Division and the University of Nebraska Office of Research and Economic
574 Development. Additionally, JRH acknowledges funding from the US National Air &

575 Space Administration (Grant #80NSSC17K0737), the US National Science Foundation
576 (EPSCoR Grant #1557417), and US National Institute of Justice (Grant #2017-IJ-CX-
577 0025), all of which indirectly supported this research through the support of research in
578 his laboratory. Funding agencies had no role in study design, data collection and
579 interpretation, or the decision to submit the work for publication.
580

581 **Conflict of Interest Statement**

582 On behalf of all authors, the corresponding author states that there is no conflict of
583 interest.
584

585 **Author Contributions**

586 JRH initiated the work and sampled field collections; RAK extracted RNA from all the
587 tissue samples and performed the laboratory work; RAK and JRH processed the
588 experimental data, analyzed the data, designed the figures, and drafted the manuscript.
589

590 **REFERENCES**

591 1. Zeilinger S, Omann M. 2007. *Trichoderma* biocontrol: signal transduction
592 pathways involved in host sensing and mycoparasitism. *Gene Regul Syst Bio*
593 **1**:227–234.
594 2. Sun Z-B, Li S-D, Ren Q, Xu J-L, Lu X, Sun M-H. 2020. Biology and applications
595 of *Clonostachys rosea*. *J Appl Microbiol* **129**:486–495.
596 3. Quandt CA, Kepler RM, Gams W, Araújo JPM, Ban S, Evans HC, Hughes D,
597 Humber R, Hywel-Jones N, Li Z, Luangsa-Ard JJ, Rehner SA, Sanjuan T, Sato

598 H, Shrestha B, Sung G-H, Yao Y-J, Zare R, Spatafora JW. 2014. Phylogenetic-
599 based nomenclatural proposals for Ophiocordycipitaceae (Hypocreales) with new
600 combinations in *Tolypocladium*. *IMA Fungus* **5**:121–134.
601 4. Currie CR, Mueller UG, Malloch D. 1999. The agricultural pathology of ant fungus
602 gardens. *Proc Natl Acad Sci U S A* **96**:7998–8002.
603 5. Reynolds HT, Currie CR. 2004. Pathogenicity of *Escovopsis weberi*: the parasite
604 of the attine ant-microbe symbiosis directly consumes the ant-cultivated fungus.
605 *Mycologia* **96**:955–959.
606 6. Rogerson CT, Samuels GJ. 1994. Agaricicolous species of *Hypomyces*.
607 *Mycologia* **86**:839–866.
608 7. Zugmaier W, Bauer R, Oberwinkler F. 1994. Mycoparasitism of some *Tremella*
609 species. *Mycologia* **86**:49–56.
610 8. Zamora JC, Millanes AM, Rico VJ, Pérez-Ortega S. 2015. Understanding
611 lichenicolous heterobasidiomycetes: new taxa and reproductive innovations in
612 *Tremella* s.l. Mycologia **108**:381–396.
613 9. Redhead SA, Ammirati JF, Walker GR, Norvell LL, Puccio MB. 1994.
614 *Squamanita contortipes*, the Rosetta Stone of a mycoparasitic agaric genus. *Can*
615 *J Bot* **72**:1814–1828.
616 10. Griffith GW, Piotr Gajda K, Detheridge AP, Douglas B, Bingham J, Turner A,
617 Bowmaker V, Evans DA, McAdoo WG, Dentinger BTM. 2019. Strangler
618 unmasked: Parasitism of *Cystoderma amianthinum* by *Squamanita paradoxa* and
619 *S. pearsonii*. *Fungal Ecol* **39**:131–141.

620 11. Weber R, Webster J. 1996. *Volvariella surrecta*: An uncommon mycoparasite.
621 *Mycologist* **10**:160.
622 12. Both EE. 2006. Personal encounters with the parasitic bolete. *Field Mycol* **7**:1–7.
623 13. Buller A. 1924. *Researches on Fungi.* Longmans, London, UK.
624 14. Watling R. 1974. Dimorphism in *Entoloma abortivum*. *Bull Soc Linn Lyon, Num*
625 *Spec* **43**:449–470.
626 15. Baumgartner K, Coetzee MPA, Hoffmeister D. 2011. Secrets of the subterranean
627 pathosystem of *Armillaria*. *Mol Plant Pathol* **12**:515–534.
628 16. Koch RA, Wilson AW, Séné O, Henkel TW, Aime MC. 2018. Resolved phylogeny
629 and biogeography of the root pathogen *Armillaria* and its gasteroid relative,
630 *Guyanagaster*. *BMC Evol Biol* **17**:33.
631 17. Lindner Czederpiltz DL, Volk TJ, Burdsall HH, Jr. 2001. Field observations and
632 inoculation experiments to determine the nature of the carpophoroids associated
633 with *Entoloma abortivum* and *Armillaria*. *Mycologia* **93**:841–851.
634 18. Druzhinina IS, Seidl-Seiboth V, Herrera-Estrella A, Horwitz BA, Kenerley CM,
635 Monte E, Mukherjee PK, Zeilinger S, Grigoriev IV, Kubicek CP. 2011.
636 *Trichoderma*: the genomics of opportunistic success. *Nat Rev Microbiol* **9**:749–
637 759.
638 19. Quandt CA, Di Y, Elser J, Jaiswal P, Spatafora JW. 2016. Differential expression
639 of genes involved in host recognition, attachment, and degradation in the
640 mycoparasite *Tolypocladium ophioglossoides*. *G3* **6**:731–741.
641 20. Karlsson M, Atanasova L, Jensen DF, Zeilinger S. 2017. Necrotrophic
642 mycoparasites and their genomes. *Microbiol Spectr* **5**:FUNK-0016-2016.

643 21. Ross-Davis AL, Stewart JE, Hanna JW, Kim MS, Knaus BJ, Cronn R, Rai H,
644 Richardson BA, McDonald GI, Klopfenstein NB. 2013. Transcriptome of an
645 *Armillaria* root disease pathogen reveals candidate genes involved in host
646 substrate utilization at the host–pathogen interface. *For Pathol* **43**:468–477.
647 22. Sipos G, Prasanna AN, Walter MC, O'Connor E, Bálint B, Krizsán K, Kiss B,
648 Hess J, Varga T, Slot J, Riley R, Bóka B, Rigling D, Barry K, Lee J, Mihaltcheva
649 S, LaButti K, Lipzen A, Waldron R, Moloney NM, Sperisen C, Kredics L,
650 Vágvölgyi C, Patrignani A, Fitzpatrick D, Nagy I, Doyle S, Anderson JB, Grigoriev
651 IV, Güldener U, Münsterkötter M, Nagy L. 2017. Genome expansion and lineage-
652 specific genetic innovations in the forest pathogenic fungi *Armillaria*. *Nat Ecol*
653 *Evol* **1**:1931–1941.
654 23. Dodd RB, Drickamer K. 2001. Lectin-like proteins in model organisms:
655 implications for evolution of carbohydrate-binding activity. *Glycobiology* **11**:71R–
656 79R.
657 24. Inbar J, Chet I. 1992. Biomimics of fungal cell-cell recognition by use of lectin-
658 coated nylon fibers. *J Bacteriol* **174**:1055–1059.
659 25. Inbar J, Chet I. 1996. The role of lectins in recognition and adhesion of the
660 mycoparasitic fungus *Trichoderma* spp. to its host. *Adv Exp Med Biol* **408**:229–
661 231.
662 26. Neethling D, Nevalainen H. 1996. Mycoparasitic species of *Trichoderma* produce
663 lectins. *Can J Microbiol* **42**:141–146.
664 27. Schubert M, Bleuler-Martinez S, Butschi A, Wälti MA, Egloff P, Stutz K, Yan S,
665 Wilson IBH, Hengartner MO, Aebi M, Allain FHT, Künzler M. 2012. Plasticity of

666 the β-trefoil protein fold in the recognition and control of invertebrate predators
667 and parasites by a fungal defense system. *PLoS Pathog* **8**:e1002706.
668 28. Latgé JP, Kobayashi H, Debeaupuis JP, Diaquin M, Sarfati J, Wieruszeski JM,
669 Parra E, Bouchara JP, Fournet B. 1994. Chemical and immunological
670 characterization of the extracellular galactomannan of *Aspergillus fumigatus*.
671 *Infect Immun* **62**:5424–5433.
672 29. Cessna SG, Sears VE, Dickman MB, Low PS. 2000. Oxalic acid, a pathogenicity
673 factor for *Sclerotinia sclerotiorum*, suppresses the oxidative burst of the host
674 plant. *Plant Cell* **12**:2191–2200.
675 30. Dumas MT, Boyonoski N, Jeng RS. 1989. Oxalic acid production by species of
676 *Armillaria* in the boreal mixedwood forest. In: Proc. 7th International Conference
677 on Root and Butt Rots. 9–16 Aug. 1988, Vernon and Victoria, British Columbia.
678 Forestry Canada, Pacific Forestry Centre, Victoria, B.C. 680 p. 593–601.
679 31. Munir E, Jun Yoon J, Tokimatsu T, Hattori T, Shimada M. 2001. A physiological
680 role for oxalic acid biosynthesis in the wood-rotting basidiomycete *Fomitopsis*
681 *palustris*. *Proc Natl Acad Sci U S A* **98**:11126–11130.
682 32. Wang Y, Wang Y. 2020. Oxalic acid metabolism contributes to full virulence and
683 pycnidial development in the poplar canker fungus *Cytospora chrysosperma*.
684 *Phytopathology* **110**:1319–1325.
685 33. Wei SJ, Li GQ, Jiang DH, Wang DB. 2004. Effect of oxalic acid on spore
686 germination and mycelial growth of the mycoparasite *Coniothyrium minitans*.
687 *Acta Phytopathol Sin* **34**:199–203.

688 34. Ren L, Li GQ, Han YC, Jiang DH, Huang HC. 2007. Degradation of oxalic acid by
689 *Coniothyrium minitans* and its effects on production and activity of β-1,3-
690 glucanases of this mycoparasite. *Biol Control* **43**:1–11.
691 35. Ren L, Li GQ, Jiang DH. 2010. Characterization of some culture factors affecting
692 oxalate degradation by the mycoparasite *Coniothyrium minitans*. *J Appl Microbiol*
693 **108**:173–180.
694 36. Zeng L-M, Zhang J, Han Y-C, Yang L, Wu M-d, Jiang D-H, Chen W, Li G-Q.
695 2014. Degradation of oxalic acid by the mycoparasite *Coniothyrium minitans*
696 plays an important role in interacting with *Sclerotinia sclerotiorum*. *Environ*
697 *Microbiol* **16**:2591–2610.
698 37. Dubey M, Jensen DF, Karlsson M. 2015. The ABC transporter ABCG29 is
699 involved in H_2O_2 tolerance and biocontrol traits in the fungus *Clonostachys rosea*.
700 *Mol Genet Genom* **291**:677–686.
701 38. Ruocco M, Lanzuise S, Vinale F, Marra R, Turrà, Lois Woo S, Lorito M. 2009.
702 Identification of a new biocontrol gene in *Trichoderma* atroviride: the role of an
703 ABC transporter membrane pump in the interaction with different plant-
704 pathogenic fungi. *Mol Plant Microbe In* **22**:291–301.
705 39. Zhao H, Zhou T, Xie J, Cheng J, Chen T, Jiang D, Fu Y. 2020. Mycoparasitism
706 illuminated by genome and transcriptome sequencing of *Coniothyrium minitans*,
707 an important biocontrol fungus of the plant pathogen *Sclerotinia sclerotiorum*.
708 *Microb Genom* **6**:e000345.
709 40. Nygren K, Dubey M, Zapparata A, Iqbal M, Tzelepis GD, Brandström Durling M,
710 Funck Jensen D, Karlsson M. 2018. The mycoparasitic fungus *Clonostachys*

711 *rosea* responds with both common and specific gene expression during
712 interspecific interactions with fungal prey. *Evol Appl* **11**:931–949.
713 41. Atanasova L, Le Crom S, Gruber S, Coulpier F, Seidl-Seiboth V, Kubick CP,
714 Druzhinina IS. 2013. Comparative transcriptomics reveals different strategies of
715 *Trichoderma* mycoparasitism. *BMC Genom* **14**:121.
716 42. Cha JY, Igarashi T. 1996. Biological species of *Armillaria* and their mycoparasitic
717 associations with *Rhodophyllus abortivus* in Hokkaido. *Mycoscience* **37**:25–30.
718 43. Tregear JW, Roberts LM. 1992. The lectin gene family of *Ricinus communis*:
719 Cloning of a functional ricin gene and three lectin pseudogenes. *Plant Mol Biol*
720 **18**:515–525.
721 44. Pohleven J, Obermajer N, Sabotič J, Anžlovar S, Sepčić K, Kos J, Kralj B,
722 Štrukelj B, Brzin J. 2009. Purification, characterization and cloning of a ricin B-
723 like lectin from mushroom *Clitocybe nebularis* with antiproliferative activity
724 against human leukemic T cells. *Biochim Biophys Acta Gen Subj* **1790**:173–181.
725 45. Žurga S, Pohleven J, Renko M, Bleuler-Martínez S, Sosnowski P, Turk D,
726 Künzler M, Kos J, Sabotič J. 2014. A novel beta-trefoil lectin from the parasol
727 mushroom (*Macrolepiota procera*) is nematotoxic. *FEBS J* **281**:3489–3506.
728 46. Bovi M, Cenci L, Perduca M, Capaldi S, Carrizo ME, Civiero L, Chiarelli LR,
729 Galliano M, Monaco HL. 2013. BEL beta-trefoil: a novel lectin with antineoplastic
730 properties in king bolete (*Boletus edulis*) mushrooms. *Glycobiology* **23**:578–592.
731 47. Sabotič J, Ohm RA, Künzler M. 2016. Entomotoxic and nematotoxic lectins and
732 protease inhibitors from fungal fruiting bodies. *Appl Microbiol Biotechnol* **100**:91–
733 111.

734 48. Pohleven J, Renko M, Magister S, Smith DF, Künzler M, Strukelj B, Turk D, Kos
735 J, Sabotič J. 2012. Bivalent carbohydrate binding is required for biological activity
736 of *Clitocybe nebularis* lectin (CNL), the N, N'-diacetyllactosediamine
737 (GalNAcbeta1-4GlcNAc, LacdiNAc)-specific lectin from basidiomycete *C.*
738 *nebularis*. *J Biol Chem* **287**:10602–10612.
739 49. Latgé JP. 2007. The cell wall: a carbohydrate armour for the fungal cell. *Mol*
740 *Microbiol* **66**:279–290.
741 50. de Man TJ, Stajich JE, Kubicek CP, Teiling C, Chenthamara K, Atanasova L,
742 Druzhinina IS, Levenkova N, Birnbaum SS, Barribeau SM, Bozick BA, Suen G,
743 Currie CR, Gerardo NM. 2016. Small genome of the fungus *Escovopsis weberi*, a
744 specialized disease agent of ant agriculture. *Proc Natl Acad Sci U S A* **113**:3567–
745 3572.
746 51. Kubicek CP, Herrera-Estrella A, Seidl-Seiboth V, Martinez DA, Druzhinina IS,
747 Thon M, Zeilinger S, Casas-Flores S, Horwitz BA, Mukherjee PK, Mukherjee M,
748 Kredics L, Alcaraz LD, Aerts A, Antal Z, Atanasova L, Cervantes-Badillo MG,
749 Challacombe J, Chertkov O, McCluskey K, Coulpier F, Deshpande N, von
750 Döhren H, Ebbole DJ, Esquivel-Naranjo EU, Fekete E, Flipphi M, Glaser F,
751 Gómez-Rodríguez EY. Gruber S, Han C, Henrissat B, Hermosa R, Hernández-
752 Oñate M, Karaffa L, Kosti I, Le Crom S, Lindquist E, Lucas S, Lübeck M, Lübeck
753 PS, Margeot A, Metz B, Misra M, Nevalainen H, Omann M, Packer N, Perrone G,
754 Uresti-Rivera EE, Salamov A, Schmoll M, Seiboth B, Shapiro H, Sukno S,
755 Tamayo-Ramos JA, Tisch D, Wiest A, Wilkinson HH, Zhang M, Coutinho PM,
756 Kenerley CM, Monte E, Baker SE, Grigoriev IV. 2011. Comparative genome

757 sequence analysis underscores mycoparasitism as the ancestral life style of
758 *Trichoderma*. *Genome Biol* **12**:R40.
759 52. Ihrmark K, Asmail N, Ubhayasekera W, Melin P, Stenlid J, Karlsson M. 2010.
760 Comparative molecular evolution of *Trichoderma* chitinases in response to
761 mycoparasitic interactions. *Evol Bioinform* **6**:1–26.
762 53. Xie BB, Qin QL, Shi M, Chen LL, Shu YL, Luo Y, Wang XW, Rong JC, Gong ZT,
763 Li D, Sun CY, Liu GM, Dong XW, Pang XH, Huang F, Liu W, Chen XL, Zhou BC,
764 Zhang YZ, Song ZY. 2014. Comparative genomics provides insights into
765 evolution of *Trichoderma* nutrition style. *Genome Biol Evol* **6**:379–390.
766 54. Miyauchi S, Kiss E, Kuo A, Drula E, Kohler A, Sánchez-García M, Morin E,
767 Andreopoulos B, Barry KW, Bonito G, Buée M, Carver A, Chen C, Cichocki N,
768 Clum A, Culley D, Crous PW, Fauchery L, Girlanda M, Hayes RD, Kéri Z, LaButti
769 K, Lipzen A, Lombard V, Magnuson J, Maillard F, Murat C, Nolan M, Ohm RA,
770 Pangilinan J, Pereira MF, Perotto S, Peter M, Pfister S, Riley R, Sitrit Y, Stielow
771 JB, Szöllősi G, Žifčáková L, Štursová M, Spatafora JW, Tedersoo L, Vaario LM,
772 Yamada A, Yan M, Wang P, Xu J, Bruns T, Baldrian P, Vilgalys R, Dunand C,
773 Henrissat B, Grigoriev IV, Hibbett D, Nagy LG, Martin FM. 2020. Large-scale
774 genome sequencing of mycorrhizal fungi provides insights into the early evolution
775 of symbiotic traits. *Nat Commun* **11**:5125.
776 55. Ruiz-Dueñas FJ, Barrasa JM, Sánchez-García M, Camarero S, Miyauchi S,
777 Serrano A, Linde D, Babiker R, Drula E, Ayuso-Fernández I, Pacheco R, Padilla
778 G, Ferreira P, Barriuso J, Kellner H, Castanera R, Alfaro M, Ramirez L, Pisabarro
779 AG, Riley R, Kuo A, Andreopoulos W, LaButti K, Pangilinan J, Tritt A, Lipzen A,

780 He G, Yan M, Ng V, Grigoriev IV, Cullen D, Martin F, Rosso MN, Henrissat B,
781 Hibbett D, Martínez AT. 2020. Genomic analysis enlightens Agaricales lifestyle
782 evolution and increasing peroxidase diversity. *Mol Biol Evol*
783 doi:10.1093/molbev/msaa301.
784 56. Steindorff AS, Carver A, Calhoun S, Stillman K, Liu H, Lipzen A, He G, Yan M,
785 Pangilinan J, LaButti K, Ng V, Bruns TD, Grigoriev IV. 2020. Comparative
786 genomics of pyrophilous fungi reveals a link between fire events and
787 developmental genes. *Environ Microbiol* **23**:99–109.
788 57. Han Y-C, Li G-Q, Yang L, Jiang D-H. 2011. Molecular cloning, characterization
789 and expression analysis of a *pacC* homolog in the mycoparasite *Coniothyrium*
790 *minitans. World J Microbiol Biotechnol* **27**:381–391.
791 58. Ahrendt SR, Quandt CA, Ciobanu D, Clum A, Salamov A, Andreopoulos B,
792 Cheng J-F, Woyke T, Pelin A, Henrissat B, Reynolds NK, Benny GL, Smith ME,
793 James TY, Grigoriev IV. 2018. Leveraging single-cell genomics to expand the
794 fungal tree of life. *Nat Microbiol* **3**:1417–1428.
795 59. Palmer JM, Drees KP, Foster JT, Lindner DL. 2018. Extreme sensitivity to
796 ultraviolet light in the fungal pathogen causing white-nose syndrome of bats. *Nat*
797 *Commun* **9**:35.
798 60. Agerer R, Waller K. 1993. Mycorrhizae of *Entoloma saepium*: parasitism or
799 symbiosis? *Mycorrhiza* **3**:145–154.
800 61. Kobayashi H, Hatano K. 2001. A morphological study of the mycorrhiza of
801 *Entoloma clypeatum* f. *hybridum* on *Rosa multiflora*. *Mycoscience* **42**:83–90.

802 62. Shishikura M, Takemura Y, Sotome K, Maekawa N, Nakagiri A, Endo N. 2021.
803 Four mycelial strains of *Entoloma clypeatum* species complex form
804 ectomycorrhiza-like roots with *Pyrus betulifolia* seedlings in vitro, and one
805 develops fruiting bodies 2 months after inoculation. *Mycorrhiza* **31**:31–42.
806 63. Kohler A, Kuo A, Nagy LG, Morin E, Barry KW, Buscot F, Canbäck B, Choi C,
807 Cichocki N, Clum A, Colpaert J, Copeland A, Costa MD, Doré J, Floudas D, Gay
808 G, Girlanda M, Henrissat B, Herrmann S, Hess J, Högberg N, Johansson T,
809 Khouja H-R, LaButti K, Lahrmann U, Levasseur A, Lindquist EA, Lipzen A,
810 Marmeisse R, Martino E, Murat C, Ngan CY, Nehls U, Plett JM, Pringle A, Ohm
811 RA, Perotto S, Peter M, Riley R, Rineau F, Ruytinx J, Salamov A, Shah F, Sun
812 H, Tarkka M, Tritt A, Veneault-Fourrey C, Zuccaro A, Mycorrhizal Genomics
813 Initiative Consortium, Tunlid A, Grigoriev IV, Hibbett DS, Martin F. 2015.
814 Convergent losses of decay mechanisms and rapid turnover of symbiosis genes
815 in mycorrhizal mutualists. *Nat Genet* **47**:410–415.
816 64. Noordeloos ME. 1987. *Entoloma* (Agaricales) in Europe. *Beih Nova Hedwigia*
817 **91**:1–419.
818 65. Noordeloos ME. 1993. Studies in *Clitopilus* (Basidiomycetes, Agaricales) in
819 Europe. *Persoonia* **15**:241–248.
820 66. Collins C, Keane TM, Turner DJ, O'Keeffe G, Fitzpatrick DA, Doyle S. 2013.
821 Genomic and proteomic dissection of the ubiquitous plant pathogen, *Armillaria*
822 *mellea*: Toward a new infection model system. *J Proteome Res* **12**:2552–2570.

823 67. Strickler SR, Bombarely A, Mueller LA. 2012. Designing a transcriptome next-
824 generation sequencing project for a nonmodel plant species. *Am J Bot* **99**:257–
825 266.
826 68. Fukuda M, Nakashima E, Hayashi K, Nagasawa E. 2003. Identification of the
827 biological species of *Armillaria* associated with *Wynnea* and *Entoloma abortivum*
828 using PCR-RFLP analysis of the intergenic region (IGR) of ribosomal DNA.
829 *Mycol Res* **107**:1435–1441.
830 69. Schuierer S, Carbone W, Knehr J, Petitjean V, Fernandez A, Sultan M, Roma G.
831 2017. A comprehensive assessment of RNA-seq protocols for degraded and low-
832 quantity samples. *BMC Genom* **18**:1–13.
833 70. Crusoe MR, Alameldin HF, Awad S, Boucher E, Caldwell A, Cartwright R,
834 Charbonneau A, Constantinides B, Edvenson G, Fay S, Fenton J, Fenzl T, Fish
835 J, Garcia-Gutierrez L, Garland P, Gluck J, González I, Guermond S, Guo J,
836 Gupta A, Herr JR, Howe A, Hyer A, Härpfer A, Irber L, Kidd R, Lin D, Lippi J,
837 Mansour T, McA'Nulty P, McDonald E, Mizzi J, Murray KD, Nahum JR, Nanlohy
838 K, Nederbragt AJ, Ortiz-Zuazaga H, Ory J, Pell J, Pepe-Ranney C, Russ ZN,
839 Schwarz E, Scott C, Seaman J, Sievert S, Simpson J, Skennerton CT, Spencer
840 J, Srinivasan R, Standage D, Stapleton JA, Steinman SR, Stein J, Taylor B,
841 Trimble W, Wiencko HL, Wright M, Wyss B, Zhang Q, zyme e, Brown CT. 2015.
842 The khmer software package: enabling efficient nucleotide sequence analysis.
843 *F1000Res* **4**:900.
844 71. Grabherr MG, Haas BJ, Yassour M, Levin JZ, Thompson DA, Amit I, Adiconis X,
845 Fan L, Raychowdhury R, Zeng Q, Chen Z, Mauceli E, Hacohen N, Gnirke A,

846 Rhind N, di Palma F, Birren BW, Nusbaum C, Lindblad-Toh K, Friedman N,
847 Regev A. 2011. Trinity: reconstructing a full-length transcriptome without a
848 genome from RNA-Seq data. *Nat Biotechnol* **29**:644–652.
849 72. Mikheenko A, Prjibelski A, Saveliev V, Antipov D, Gurevich A. 2018. Versatile
850 genome assembly evaluation with QUAST-LG. *Bioinformatics* **34**:i142–i150.
851 73. Seppey M, Manni M, Zdobnov EM. 2019. BUSCO: Assessing genome assembly
852 and annotation completeness. In: Kollmar M (eds) Gene Prediction. Methods in
853 Molecular Biology, vol 1962. Humana, New York, NW.
854 74. Langmead B, Salzberg SL. 2012. Fast gapped-read alignment with Bowtie 2. *Nat*
855 *Methods* **9**:357–359.
856 75. Li B, Dewey CN. 2011. RSEM: accurate transcript quantification from RNA-Seq
857 data with or without a reference genome. *BMC Bioinform* **12**:323.
858 76. Robinson MD, McCarthy DJ, Smyth GK. 2010. edgeR: a Bioconductor package
859 for differential expression analysis of digital gene expression data. *Bioinformatics*
860 **26**:139–140.
861 77. Robinson MD, Oshlack A. 2010. A scaling normalization method for differential
862 expression analysis of RNA-seq data. *Genome Biol* **11**:R25.
863 78. Li H, Handsaker B, Wysoker A, Fennell T, Ruan J, Homer N, Marth G, Abecasis
864 G, Durbin R, 1000 Genome Project Data Processing Subgroup. 2009. The
865 Sequence Alignment/Map format and SAMtools. *Bioinformatics* **25**:2078–2079.
866 79. Bryant DM, Johnson K, DiTommaso T, Tickle T, Brian Couger M, Payzin-Dogru
867 D, Lee TJ, Leigh ND, Kuo T-H, Davis FG, Bateman J, Bryant S, Guzikowski AR,
868 Tsai SL, Coyne S, Ye WW, Freeman RM, Jr, Peshkin L, Tabin CJ, Regev A,

869 Haas BJ, Whited JL. 2017. A tissue-mapped azolotl de novo transcriptome
870 enables identification of limb regeneration factors. *Cell Rep* **18**:P762–P776.
871 80. Camacho C, Coulouris G, Avagyan V, Ma N, Papadopoulos J, Bealer K, Madden
872 TL. 2009. BLAST+: architecture and application. *BMC Bioinform* **10**:421.
873 81. Wheeler TJ, Eddy SR. 2013. nhmmer: DNA homology search with profile HMMs.
874 *Bioinformatics* **29**:3487–3489.
875 82. Finn RD, Bateman A, Clements J, Coggill P, Eberhardt RY, Eddy SR, Heger A,
876 Hetherington K, Holm L, Mistry J, Sonnhammer ELL, Tate J, Punta M. 2014.
877 Pfam: the protein families database. *Nucleic Acids Res* **42**:D222–D230.
878 83. Ashburner M, Ball CA, Blake JA, Botstein D, Butler H, Cherry JM, Davis AP,
879 Dolinski K, Dwight SS, Eppig JT, Harris MA, Hill DP, Issel-Tarver L, Kasarskis A,
880 Lewis S, Matese JC, Richardson JE, Ringwald M, Rubin GM, Sherlock G. 2000.
881 Gene Ontology: tool for the unification of biology. *Nat Genet* **25**:25–29.
882 84. Kanehisa M, Goto S. 2000. KEGG: Kyoto Encyclopedia of Genes and Genomes.
883 *Nucleic Acids Res* **28**:27–30.
884 85. Kanehisa M. 2019. Toward understanding the origin and evolution of cellular
885 organisms. *Protein Sci* **28**:1947–1951.
886 86. Kanehisa M, Furumichi M, Sato Y, Ishiguro-Watanabe M, Tanabe M. 2021.
887 KEGG: integrating viruses and cellular organisms. *Nucleic Acids Res* **49**:D545–
888 D551.
889 87. Zhang H, Yohe T, Huang L, Entwistle S, Wu P, Yang Z, Busk PK, Xu Y, Yin Y.
890 2018. dbCAN2: a meta server for automated carbohydrate-active enzyme
891 annotation. *Nucleic Acids Res* **46**:W95–W101.

892 88. Blin K, Shaw S, Steinke K, Villebro R, Ziemert N, Yup Lee S, Medema MH,
893 Weber T. 2019. antiSMASH 5.0: updates to the secondary metabolite genome
894 mining pipeline. *Nucleic Acids Res* **47**:W81–W87.
895 89. Bengtsson-Palme J, Ryberg M, Hartmann M, Branco S, Wang Z, Godhe A, De
896 Wit P, Sánchez-García M, Ebersberger I, de Sousa F, Amend A, Jumpponen A,
897 Unterseher M, Kristiansson E, Abarenkov K, Bertrand YJK, Sanli K, Eriksson KM,
898 Vik U, Veldre V, Nilsson RH. 2013. Improved software detection and extraction of
899 ITS1 and ITS2 from ribosomal ITS sequences of fungi and other eukaryotes for
900 analysis of environmental sequencing data. *Methods Ecol Evol* **4**:914–919.
901 90. Slater GSC, Birney E. 2005. Automated generation of heuristics for biological
902 sequence comparison. *BMC Bioinformatics* **6**:31.
903 91. Floudas D, Held BW, Riley R, Nagy LG, Koehler G, Ransdell AS, Younus H,
904 Chow J, Chiniquy J, Lipzen A, Tritt A, Sun H, Haridas S, LaButtie K, Ohm RA,
905 Kües U, Blanchette RA, Grigoriev IV, Minto RE, Hibbett DS. 2015. Evolution of
906 novel wood decay mechanisms in Agaricales revealed by the genome
907 sequences of *Fistulina hepatica* and *Cylindrobasidium torrendii*. *Fungal Genet*
908 *Biol* **76**:78–92.
909 92. Koch RA, Yoon GM, Arayal UK, Lail K, Amirebrahimi M, LaButti K, Lipzen A,
910 Riley R, Barry K, Henrissat B, Grigoriev IV, Herr JR, Aime MC. 2021. Symbiotic
911 nitrogen fixation in the reproductive structures of a basidiomycete fungus. *Curr*
912 *Biol* **31**:3905–3914.
913 93. Katoh K, Standley DM. 2013. MAFFT multiple sequence alignment software
914 version 7: improvements in performance and usability. *Mol Biol Evol* **30**:772–780.

915 94. Castresana J. 2000. Selection of conserved blocks from multiple alignments for
916 their use in phylogenetic analysis. *Mol Biol Evol* **17**:540–552.
917 95. Kozlov AM, Darriba D, Flouri T, Morel B, Stamatakis A. 2019. RAxML-NG: a fast,
918 scalable and user-friendly tool for maximum likelihood phylogenetic inference.
919 *Bioinformatics* **35**:4453–4455.
920 96. Guo T, Wang HC, Xue WQ, Zhao J, Yang ZL. 2016. Phylogenetic analyses of
921 *Armillaria* reveal at least 15 phylogenetic lineages in China, seven of which are
922 associated with cultivated *Gastrodia elata*. *PLoS One* **11**:e0154794.
923 97. Coetzee MPA, Wingfield BD, Harrington TC, Dalevi D, Coutinho TA, Wingfield
924 MJ. 2000. Geographical diversity of *Armillaria mellea* s. s. based on phylogenetic
925 analysis. *Mycologia* **92**:105–113.
926 98. Coetzee MPA, Wingfield BD, Bloomer P, Wingfield MJ. 2005. Phylogenetic
927 analyses of DNA sequences reveal species partitions amongst isolates of
928 *Armillaria* from Africa. *Mycol Res* **109**:1223–1234.
929 99. Schneider-Maunoury L, Deveau A, Moreno M, Todesco F, Belmondo S, Murat C,
930 Courty P-E, Jąkalski M, Selosse M-A. 2020. Two ectomycorrhizal truffles, *Tuber*
931 *melanosporum* and *T. aestivum*, endophytically colonise roots of non-
932 ectomycorrhizal plants in natural environments. *New Phytol* **225**:2542–2556.
933 100. Coetzee MPA, Bloomer P, Wingfield MJ, Wingfield BD. 2011. Paleogene
934 radiation of a plant pathogenic mushroom. *PLoS One* **6**:e28545.
935 101. Osmundson TW, Robert VA, Schoch CL, Baker LJ, Smith A, Robich G,
936 Mizzan L, Garbelotto MM. 2013. Filling gaps in biodiversity knowledge for

937 macrofungi: contributions and assessment of an herbarium collection DNA
938 barcode sequencing project. *PLoS One* **8**:e62419.
939 102. Kasper-Pakosz R, Pietras M, Łuczaj Ł. 2016. Wild and native plants and
940 mushrooms sold in the open-air markets of south-eastern Poland. *J Ethnobiol*
941 *Ethnomed* **12**:45.
942 103. Hughes KW, Petersen RH, Lodge DJ, Bergemann SE, Baumgartner K,
943 Tulloss RE, Lickey E, Cifuentes J. 2013. Evolutionary consequences of putative
944 intra- and interspecific hybridization in agaric fungi. *Mycologia* **105**:1577–1594.
945 104. Potyralska A, Schmidt O, Moreth U, Łakomy P, Siwecki R. 2002. rDNA-
946 ITS sequence of *Armillaria* species and a specific primer for *A. mellea*. *For Genet*
947 **9**:119–124.
948 105. Ortega A, Moreno G, Platas G, Pelaez F. 2008. A new *Armillaria mellea*
949 variant from tops of coastal sand dunes in southern Spain. *Mycotaxon* **104**:349–
950 364.
951 106. Vu D, Groenewald M, de Vries M, Gehrmann T, Stielow B, Eberhardt U,
952 Al-Hatmi A, Groenewald JZ, Cardinali G, Houbraken J, Boekhout T, Crous PW,
953 Robert V, Verkley GJM. 2019. Large-scale generation and analysis of
954 filamentous fungal DNA barcodes boosts coverage for kingdom fungi and reveals
955 thresholds for fungal species and higher taxon delimitation. *Stud Mycol* **92**:135–
956 154.
957 107. Binder M, Hibbett DS, Wang Z, Farnham WF. 2006. Evolutionary
958 relationships of *Mycaureola dilseae* (Agaricales), a basidiomycete pathogen of a
959 subtidal rhodophyte. *Am J Bot* **93**:547–556.

960 108. Haelewaters D, Dirks AC, Kappler LA, Mitchell JK, Quijada L, Vandegrift
961 R, Buyck B, Pfister DH. 2018. A preliminary checklist of fungi at the Boston
962 Harbor Islands. *Northeast Nat* **25**:45–76.
963 109. Kim M-S, Klopfenstein NB, Hanna JW, McDonald GI. 2006.
964 Characterization of North American *Armillaria* species: genetic relationships
965 determined by ribosomal DNA sequences and AFLP markers. *For Path* **36**:145–
966 164.
967 110. Schnabel G, Ash JS, Bryson PK. 2005. Identification and characterization
968 of *Armillaria tabescens* from the southeastern United States. *Mycol Res*
969 **109**:1208–1222.
970 111. Dentinger BTM, Gaya E, O'Brien H, Suz LM, Lachlan R, Díaz-Valderrama
971 JR, Koch RA, Aime MC. 2016. Tales from the crypt: genome mining from
972 fungarium specimens improves resolution of the mushroom tree of life. *Biol J*
973 *Linn Soc* **117**:11–32.
974

975

976 TABLE 1 Ten most abundant *E. abortivum* transcripts in sporocarps and carpophoroids

977

Gene	Annotation	Cond.	C (TMM)	S (TMM)	logFC	*q*-value
978 ENT_DN2762_c0_g3	Oxalate decarboxylase	C	68,724	238	-8.5	4.5×10^{-317}
979 ENT_DN1212_c0_g1	Hypothetical protein	C/S	55,939	12,590	-2.5	4.3×10^{-49}
980 ENT_DN3063_c0_g2	Oxalate decarboxylase	C	48,157	135	-8.8	0
981 ENT_DN1952_c0_g2	Acid phosphatase	C	19,999	677	-5.2	1.3×10^{-169}
982 ENT_DN4045_c1_g1	Hypothetical protein	C	19,965	3,374	-2.9	3.4×10^{-63}
983 ENT_DN5742_c0_g1	Hypothetical protein	C	11,229	23	-9.3	6.9×10^{-220}
984 ENT_DN4332_c0_g1	Hypothetical protein	C	11,038	607	-4.5	4.7×10^{-77}
985 ENT_DN1952_c0_g1	Acid phosphatase	C	10,766	673	-4.4	1.9×10^{-122}
986 ENT_DN2936_c0_g2	Hypothetical protein	C	9,212	3,686	NS	
987 ENT_DN3086_c0_g1	Hypothetical protein	C	9,076	1,563	-2.9	2.2×10^{-62}
988 ENT_DN1375_c0_g1	Trehalase	S	1,934	17,890	2.9	6.5×10^{-37}
989 ENT_DN5247_c0_g3	Hypothetical protein	S	2,718	7,204	NS	
990 ENT_DN761_c0_g2	Hypothetical protein	S	7,405	6,918	NS	
991 ENT_DN521_c0_g2	Hypothetical protein	S	6,045	6,424	NS	
992 ENT_DN852_c0_g1	Hypothetical protein	S	123	5,429	5.1	2.0×10^{-142}
993 ENT_DN3621_c0_g2	RNA polymerase	S	1,977	5,138	NS	
994 ENT_DN6707_c0_g1	Hypothetical protein	S	1,654	5,027	NS	
995 ENT_DN2379_c0_g1	TPR-like protein	S	4,862	5,017	NS	
996 ENT_DN466_c0_g1	Auxin efflux carrier	S	1,205	4,333	NS	

997 Cond.: condition in which each gene was most abundant, referring to either the carpophoroids (C) or sporocarps (S). NS: not significantly
998 differentially upregulated. Negative logFC values are significantly differentially upregulated in the carpophoroid, whereas positive values are
999 significantly differentially upregulated in the sporocarp. Transcripts discussed in the text include two oxalate decarboxylases
1000 (ENT_DN2762_c0_g3, ENT_DN3063_c0_g2), three β-trefoil-type lectins (ENT_DN4359_c0_g1, ENT_DN1877_c0_g1,
1001 ENT_DN4255_c0_g1), three ABC transporters (ENT_DN1537_c0_g1, ENT_DN189_c0_g1, ENT_DN3860_c0_G1), two chitinases
1002 (ENT_DN2096_c0_g1, ENG_DN4507_c0_g3) and 14 MFS transcripts (ENT_DN409_c0_g1, ENT_DN1954_c0_g1, ENT_DN1998_c0_g1,

1003 ENT_DN2070_c0_g1, ENT_DN2744_c0_g1, ENT_DN3292_c0_g1, ENT_DN3474_c0_g1, ENT_DN3861_c0_g1, ENT_DN3943_c0_g1,

1004 ENT_DN3943_c0_g2, ENT_DN3981_c0_g1, ENT_DN4751_c0_g2, ENT_DN6588_c0_g1, ENT_DN6695_c0_g1).

1005

1006 TABLE 2 Ten most abundant *Armillaria* transcripts in sporocarps and carpophoroids

Gene	Annotation	Cond.	C (TMM)	S (TMM)	logFC	*q*-value
ARM_DN1755_c2_g1	Cell wall galactomannoprotein	S	0	36,479	13.5	4.0×10^{-182}
ARM_DN3840_c0_g1	Serine carboxypeptidase	S	12	29,472	6.7	7.9×10^{-100}
ARM_DN22943_c1_g1	Rab geranylgeranyltransferase	S	21	18,649	5.1	3.8×10^{-89}
ARM_DN1737_c0_g1	LysM-domain-containing protein	S	0	14,557	15.9	3.0×10^{-159}
ARM_DN1699_c3_g1	Hypothetical protein	S	9	12,848	5.8	1.6×10^{-94}
ARM_DN1314_c0_g1	Chondroitin AC/alginate lyase	S	102	11,436	2.2	3.7×10^{-25}
ARM_DN20980_c0_g1	Glycopeptide	S	0	10,449	15.4	3.4×10^{-139}
ARM_DN8135_c0_g1	Rasp f 7 allergen	S	0	9,014	11.5	1.8×10^{-58}
ARM_DN4971_c0_g2	Aldehyde dehydrogenase	S	103	8,688	NS	
ARM_DN1205_c0_g1	Hypothetical protein	S/C	9,049	8,348	-4.8	2.1×10^{-74}
ARM_DN5170_c0_g1	Hypothetical protein	C	2,086	377	-7.1	6.9×10^{-150}
ARM_DN23207_c0_g2	Senescence-associated	C	1,711	2,482	-4.1	6.6×10^{-61}
ARM_DN996_c0_g1	Senescence-associated	C	1,423	1,090	-5.0	3.0×10^{-73}
ARM_DN409_c1_g1	Elongation factor 1-alpha	C	769	1,154	-4.1	4.0×10^{-155}
ARM_DN1893_c0_g1	Hypothetical protein	C	722	58	-8.3	5.3×10^{-109}
ARM_DN693_c0_g1	Hypothetical protein	C	520	840	-3.9	1.1×10^{-48}
ARM_DN1222_c0_g1	CYS3-cystathionine gamma-lyase	C	485	717	-4.1	5.5×10^{-27}
ARM_DN1146_c0_g4	Heat shock protein 70	C	431	2,361	-2.2	1.7×10^{-54}
ARM_DN3800_c0_g1	ATP synthase F1	C	300	4,686	NS	

1027 Cond.: condition in which each gene was most abundant, referring to either the carpophoroids (C) or sporocarps (S). NS: not
1028 significantly differentially upregulated. Negative logFC values are significantly differentially upregulated in the carpophoroid,
1029 whereas positive values are significantly differentially upregulated in the sporocarp. Transcripts discussed in the text were
1030 an isocitrate lyase (ARM_DN1_c7_g1), two putative senescence-associated proteins (ARM_DN23207_c0_g2,
1031 ARM_DN996_c0_g1), and a heat shock protein (ARM_DN1146_c0_g4).

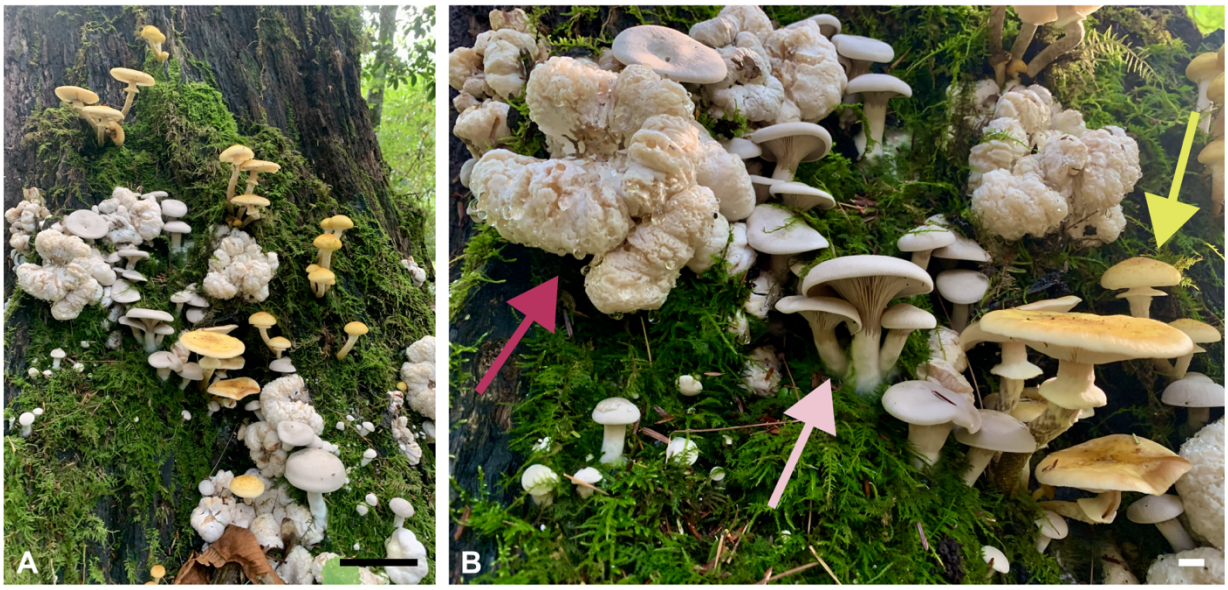

FIG 1 The components of this fungal interaction in nature. (A) All three components—*Armillaria* and *E. abortivum* sporocarps, along with carpophoroids—fruiting synchronously. (B) A close-up photo of all of the components, with an *Armillaria* sporocarp indicated by the yellow arrow, an *E. abortivum* sporocarp indicated by the light pink arrow and a carpophoroid indicated by the magenta arrow. Scale bars in A are equal to 10 cm and in B are equal to 1 cm. Photos taken by Ben Lemmond.

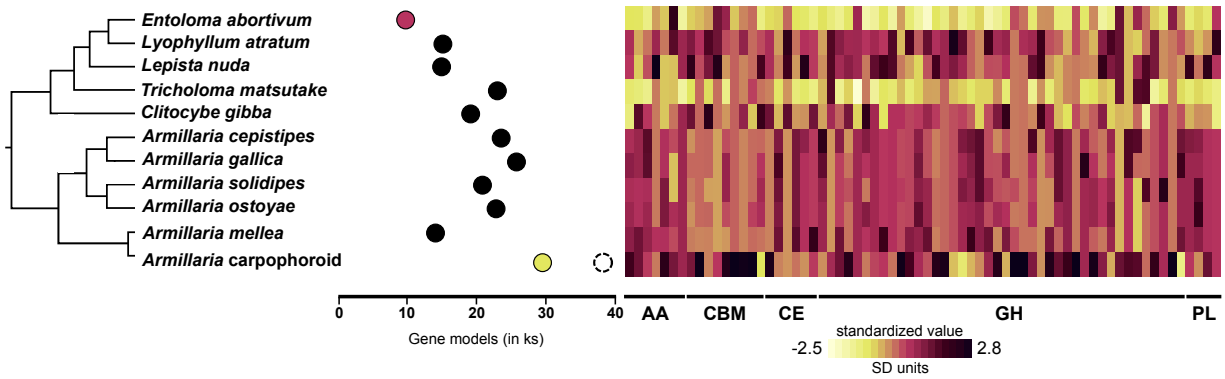

FIG 2 Number of total gene models and gene copy numbers of CAZymes. (A) A representative phylogeny based off phylogenetic evidence from (22) and (111). (B) Filled in, colored dots represent the number of fungal gene models in the transcriptomes of *Armillaria* (yellow) and *E. abortivum* (pink) generated in this study, along with those of closely related species from previously generated genomic data (filled in black dots). The dashed circle associated with the *Armillaria* carpophoroid represents the total number of identified gene models (inclusive of additional non-*Armillaria* genes), showing that nearly one quarter of the total gene models in the *Armillaria* transciptome were from organisms other than the target. (C) Heat map showing gene copy numbers of plant cell wall degrading enzymes detected in the transcriptomes of *E. abortivum* and *Armillaria*, along with other closely related species. Abbreviations: AA: Auxiliary Activities; CBM: Carbohydrate-Binding Modules; CE: Carbohydrate Esterase; GH: Glycoside Hydrolase; PL: Polysaccharide Lyase.

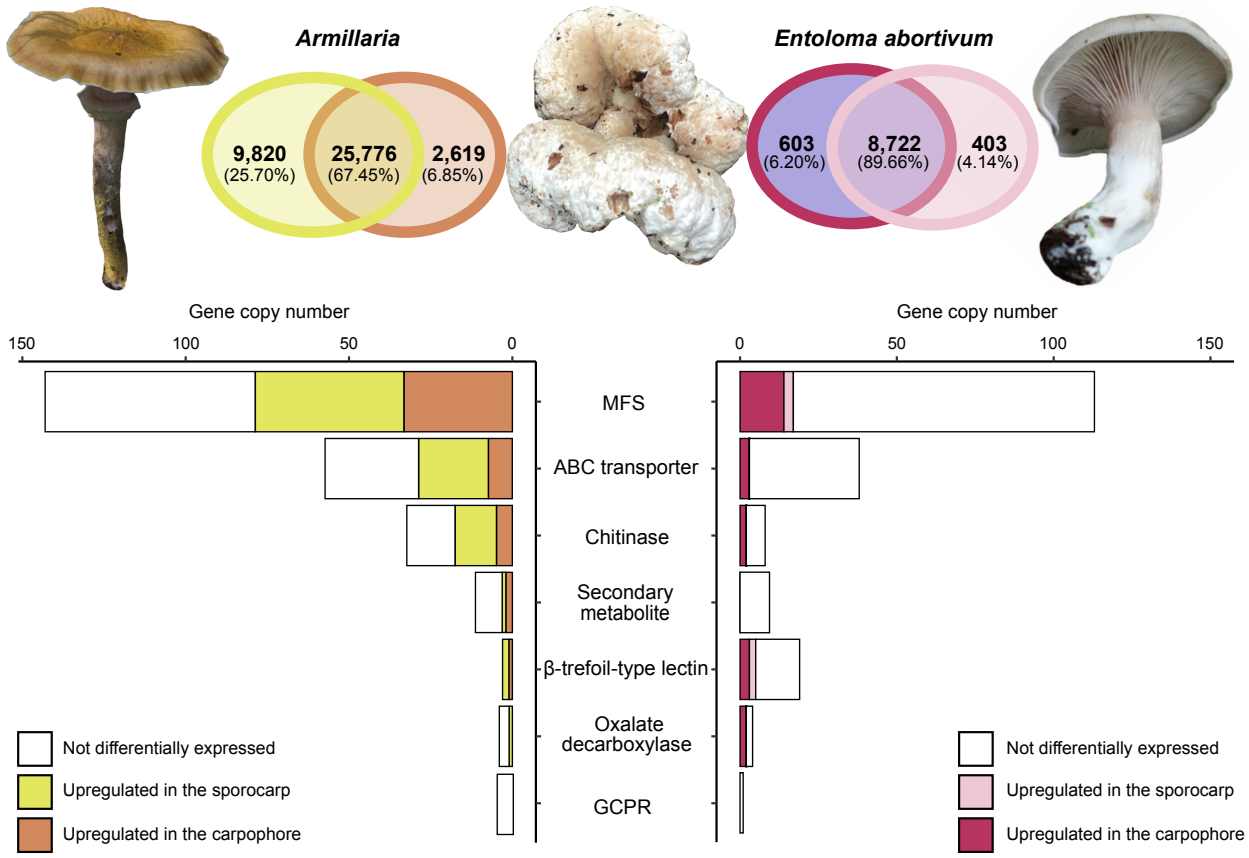

FIG 3 Differentially upregulated transcripts in the sporocarp and carpophoroid. (A) Venn diagram showing the number of differentially upregulated transcripts between the sporocarp and carpophoroid in *Armillaria* and *E. abortivum*; photo of *E. abortivum* taken by Eva Skific. (B) Bar graph showing the number of copies of genes important in mycoparasitic interactions. The white portion of the bar shows the number of these genes detected in the transcriptome but not differentially upregulated, while the darker colors (brown and purple, respectively) show the number of genes that are differentially upregulated by each species in the carpophoroid and the lighter colors (yellow and coral, respectively) show the number of these genes that are differentially upregulated by each species in their respective sporocarp.

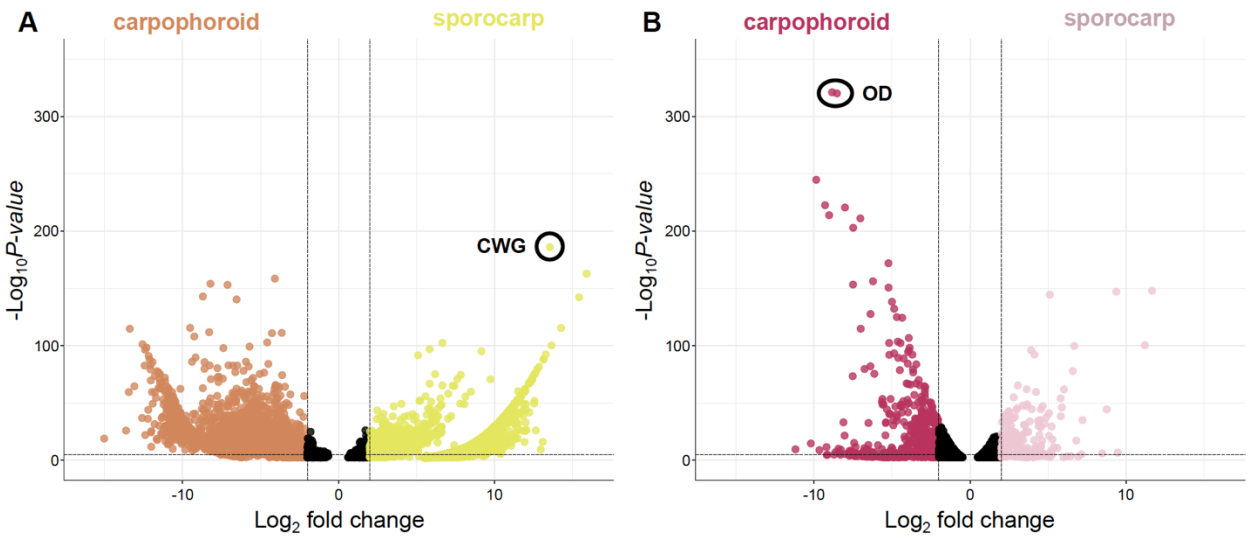

1065

1066 **FIG 4** Volcano plots. Each dot represents a transcript plotted according to its $\log_2$ fold

1067 change and the $-\log_{10}$ of its *p*-value. Transcripts with the highest statistical significance

1068 and the largest fold change will be represented by dots towards the top of the plot that

1069 are far to either the left- (carpophoroid) or right-hand (sporocarp) sides. All transcripts

1070 with a *q*-value < 0.05 are shown. Black dots represent a gene with a non-significant

1071 logFC (-2 < logFC < 2). (A) *Armillaria*. (B) *E. abortivum*. Dots with a black circle around

1072 them are annotated according to the abbreviations; OD: oxalate decarboxylase; CWG:

1073 cell wall galactomannoprotein.

1074

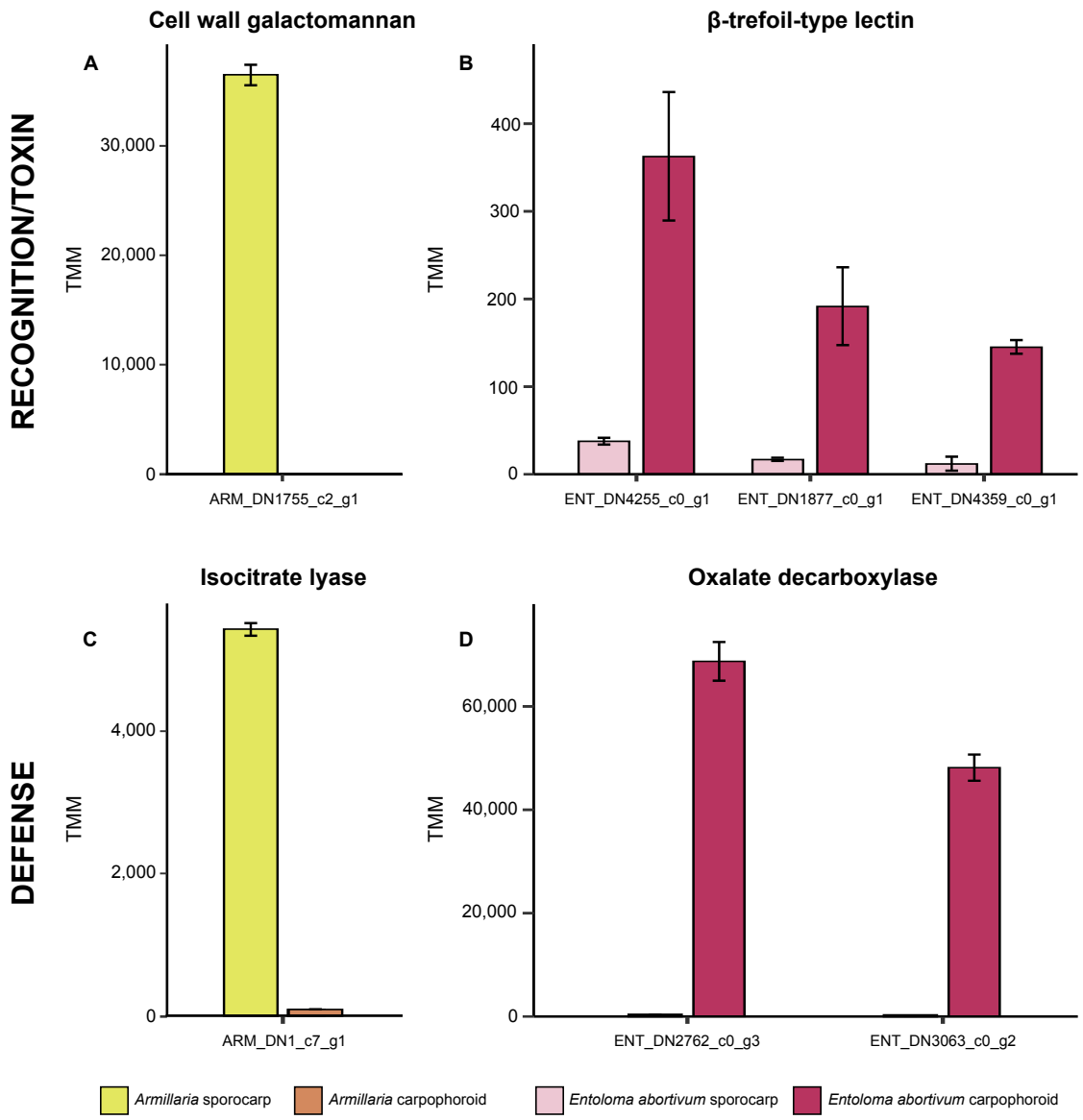

FIG 5 Genes in both *Armillaria* and *E. abortivum* that are putatively important in the recognition and defense responses during this mycoparasitic interaction. (A) An *Armillaria* cell wall galactomannan that is differentially upregulated in the sporocarp; (B) three *E. abortivum* β-trefoil-type lectins that are differentially upregulated in the carpophoroid; (C) an *Armillaria* transcript that codes for isocitrate lyase that is differentially upregulated in its sporocarps; and (D) two *E. abortivum* transcripts that code for oxalate decarboxylases that are differentially upregulated in the carpophoroids.

1083 All results are shown as means ± standard error of the mean. TMM: normalized units of

1084 trimmed mean of m-values.

1085

1086

1087

1088

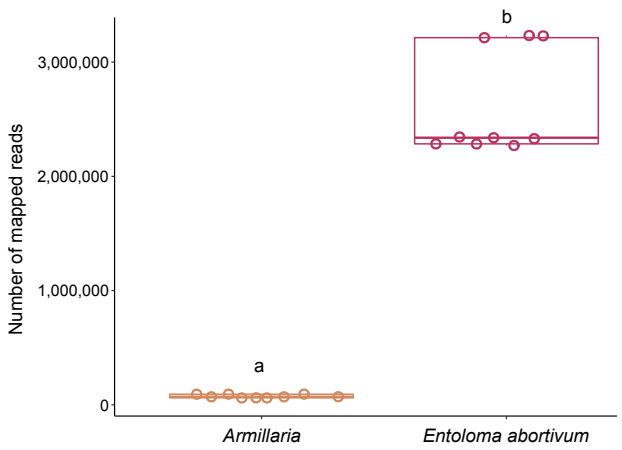

1089

1090 **FIG 6** Boxplots of number of carpophoroid reads that mapped to *Armillaria* and *E.*

1091 *abortivum* when MAPQ = 30. Individual data points are indicated for each species with

1092 an open circle. The continuous line within each box represents the mean number of

1093 mapped reads. Species labeled with different letters (a to b) have a statistically

1094 significant ($p < 0.05$) different number of mapped reads in the carpophoroid.

1095

1096

1097

A
Armillaria ostoyae
Armillaria solidipes
Armillaria cepistipes
Armillaria gallica
Armillaria mellea
USA: Michigan JRH 2446
Guyanagaster necrorhizus
Cylindrobasidium torrendii
B
Western North America
USA: California AF163597
USA: California FJ664596
USA: California FJ664595
USA: California AF163596
USA: California AF163595
USA FJ664593
USA: South Carolina AY526604
USA: South Carolina AY526602
USA: New Hampshire KT822256
USA: Georgia MG931920
USA: Virgina AY213584
USA: Virgina AY213585
USA: South Carolina AY526603
USA: South Carolina MG931929
USA: Minnesota MG931908
USA: Wisconsin AY213586
USA: Massachusetts AY789081
USA: Michigan JRH 2446
USA: New Hampshire AY213587
USA: New Hampshire AF163587
Eastern North America
USA: Massachusetts MF161188
USA: New Hampshire AF163588
USA: Tennessee MF755264
USA: Massachusetts AF163589
USA: Massachusetts AF163590
Scotland JF313749
Italy KP960556
Italy KP960538
Poland KX756392
Italy KP960550
Italy KP960558
Portugal KP960535
United Kingdom KX618581
Hungary AF163581
Italy CRA PAC2824
United Kingdom MH855148
United Kingdom KX618568
United Kingdom AF163582
United Kingdom AF163578
France MG931767
United Kingdom AF163579
Italy KP960563
France HQ232290
Italy KP960555
Iran AF163583
Ukraine JN657466
United Kingdom KX618569
Italy KP960539
Denmark MG931762
Italy KP960554
France MN660639
Italy KP960552
Slovenia KF020706
France JN657464
Poland AY848938
France AF163584
France JN657465
France AF163586
Italy FJ875692
Italy KP960564
Spain EU266545
France AF163585
Italy KP960536
Slovenia AJ250051
Sweden KY352514
United Kingdom AF163580
Italy JF907776
Italy KP960537
Italy KP960561
Italy KP960565
Italy KP960562
Italy KP960566
Europe
Japan MF095794
Spain EU266546
Italy KP960557
Azerbaijan B1458
South Korea AF163591
Japan AF163594
South Korea AF163592
South Korea AF163593
China KF032535
China KF032532
China KF032530
China KF032534
Japan KT822246
China: Sichuan KT822245
Tunisia KU863550
China: Yunnan KT822249
China KF032536
Asia
China: Zhejiang KT822254
Tibet MG931786
China: Hubei HKAS86591
China: Zhejiang KT822244
China: Yunnan MG931746
China: Lijang KP162319
China: Yunnan MG931782
China KJ643339
China: Yunnan KT822255
China: Yunnan KT822242
China: Yunnan KT822243
China: Ghizhou KT822253
China: Yunnan KT822251
Armillaria gemina IIJB 38A
Armillaria sinapina V48.5.1
Armillaria puiggarii MCA 3111
Armillaria luteobubalina VM5.2
0.03

1098

1099 **FIG 7** Phylogenetic placement of the *Armillaria* species used in this analysis. (A)
1100 Maximum likelihood phylogeny of *Armillaria* species and *Guyanagaster necrorhizus*
1101 generated from the analysis of 100 random BUSCOs. The outgroup taxon is
1102 *Cylindrobasidium torrendii*. Each node is fully supported with 100% bootstrap
1103 supported. (B) Maximum likelihood phylogeny of *Armillaria mellea* phylogenetic tree
1104 generated from the analysis of the ITS region. Branches with 70% or more bootstrap
1105 support are thickened. Outgroup taxa include *A. gemina, A. luteobubalina*, *A. puiggarii*
1106 and *A. sinapina*. The *Armillaria* specimen analyzed during this study is in bold and
1107 yellow in both phylogenies.
1108
1109